Received: 18 September 2023 | Accepted: 28 February 2024

DOI: 10.1111/pce.14879

ORIGINAL ARTICLE

Plant, Cell & Environment PC&E WILEY

Dynamics and interplay of photosynthetic regulatory processes depend on the amplitudes of oscillating light

Yuxi Niu[1] | Shizue Matsubara[1] | Ladislav Nedbal[1,2] | Dušan Lazár[2]

[1]Institute of Bio- and Geosciences/Plant Sciences, Forschungszentrum Jülich, Wilhelm-Johnen-Straße, Jülich, Germany

[2]Department of Biophysics, Faculty of Science, Palacký University, Olomouc, Czech Republic

Correspondence
Dušan Lazár, Department of Biophysics, Faculty of Science, Palacký University, Šlechtitelů 241/27, 779 00 Olomouc, Czech Republic.
Email: dusan.lazar@upol.cz

Funding information
European Regional Development Fund, Grant/Award Number: CZ.02.1.01/0.0/0.0/16_019/0000827; HORIZON EUROPE Framework Programme, Grant/Award Number: 101046451; Federal Ministry of Education and Research of Germany, Grant/Award Number: 03SF0576A

Abstract

Plants have evolved multiple regulatory mechanisms to cope with natural light fluctuations. The interplay between these mechanisms leads presumably to the resilience of plants in diverse light patterns. We investigated the energy-dependent nonphotochemical quenching (qE) and cyclic electron transports (CET) in light that oscillated with a 60-s period with three different amplitudes. The photosystem I (PSI) and photosystem II (PSII) function-related quantum yields and redox changes of plastocyanin and ferredoxin were measured in *Arabidopsis thaliana* wild types and mutants with partial defects in qE or CET. The decrease in quantum yield of qE due to the lack of either PsbS- or violaxanthin de-epoxidase was compensated by an increase in the quantum yield of the constitutive nonphotochemical quenching. The mutant lacking NAD(P)H dehydrogenase (NDH)-like-dependent CET had a transient significant PSI acceptor side limitation during the light rising phase under high amplitude of light oscillations. The mutant lacking PGR5/PGRL1-CET restricted electron flows and failed to induce effective photosynthesis control, regardless of oscillation amplitudes. This suggests that PGR5/PGRL1-CET is important for the regulation of PSI function in various amplitudes of light oscillation, while NDH-like-CET acts' as a safety valve under fluctuating light with high amplitude. The results also bespeak interplays among multiple photosynthetic regulatory mechanisms.

KEYWORDS
alternative electron transports, cyclic electron transport, fluctuating light, rapidly reversible nonphotochemical quenching, regulation

Abbreviations: AET, alternative electron transport; AL, actinic light; CET, cyclic electron transport; Chl, chlorophyll; ChlF, chlorophyll fluorescence; Cyt b6/f, cytochrome b6f complex; Fd Red, apparent relative reduction of ferredoxin; Fd, ferredoxin; Fd^{-}_{m}, maximum reduction of ferredoxin; NDH-like, chloroplast NAD(P)H dehydrogenase-like complex; NIR, near-infrared light; NPQ, nonphotochemical quenching. Multiple molecular mechanisms lead to the lowering of emission of chlorophyll fluorescence in high light; P_m, maximum oxidation of P700; P700, primary electron donor in the reaction centre of photosystem I; PAR, photosynthetically active radiation between 400 and 700 nm, measured in units µmol photons m^{-2} s^{-1}; PC Ox, apparent relative oxidation of plastocyanin; PC, plastocyanin; PC_m, maximum oxidation of plastocyanin; PGR5, proton gradient regulation 5 protein; PGRL1, proton gradient regulation-like 1 protein; pmf, proton motive force; PsbS, chloroplastic 22 kDa photosystem II protein involved in qE; PSI, photosystem I; PSII, photosystem II; qE, energy-dependent nonphotochemical quenching. It is dependent on pH of lumen and involves PsbS and/or VDE proteins; qP, the coefficient of photochemical quenching, estimating the fraction of open photosystem II centres (with Q_A oxidised) based on a puddle model for the photosystem II units; SP, multiple-turnovers saturation pulse; TM, thylakoid membrane; VDE, violaxanthin de-epoxidase enzyme; Y(I), the effective photochemical quantum yield of photosystem I; Y(II), the effective photochemical quantum yield of photosystem II; Y(NA), The quantum yield of nonphotochemical energy dissipation in photosystem I due to acceptor side limitation; Y(ND), the quantum yield of nonphotochemical energy dissipation in photosystem I due to donor side limitation; Y(NO), the quantum yield of the constitutive (always present) nonphotochemical quenching; Y(NPQ), the quantum yield of the regulatory (light-induced) nonphotochemical quenching.

1 | INTRODUCTION

Plants grow in light that is perpetually changing due to diurnal and seasonal alternations, varying cloudiness, moving canopy and other factors (Morales & Kaiser, 2020; Smith & Berry, 2013). Light fluctuations have a wide range of characteristic frequencies and irradiance levels. For instance, the frequency caused by wind-driven leaf flutter (Durand & Robson, 2023; Roden & Pearcy, 1993) is several orders of magnitude higher than the frequency caused by moving clouds or the sun's position in the sky relative to gaps in the vegetation (Chazdon & Pearcy, 1991; Way & Pearcy, 2012). To maintain photosynthesis efficiency in such diverse fluctuating light environments, plants have developed multiple regulatory mechanisms (Allahverdiyeva et al., 2015; Gjindali et al., 2021; Kaiser et al., 2018; Kono & Terashima, 2014). These mechanisms enable plants to adjust their photosynthetic apparatus and energy metabolism to a wide range of changes in light quantity and duration.

An important role is played by the energy-dependent (qE) nonphotochemical quenching (NPQ) that protects photosystem II (PSII) by mitigating overexcitation (Demmig-Adams et al., 2014; Kromdijk et al., 2016; Roach & Krieger-Liszkay, 2012; Ruban, 2016; Ware et al., 2015). The importance of the qE-dependent protection has been demonstrated also in fluctuating light conditions (Ikeuchi et al., 2014; Külheim et al., 2002; Müller et al., 2001; Steen et al., 2020). The qE relies on two protective responses, one involving the violaxanthin de-epoxidase (VDE) (Demmig-Adams, 1990; Gilmore, 1997; Jahns & Holzwarth, 2012; Niyogi et al., 1998) and the other involving protonation of the PsbS protein (Li et al., 2000; Li et al., 2002). Both processes are activated by low luminal pH and their activations are independent on each other (Holzwarth et al., 2006; Li et al., 2000).

Cyclic electron transport around PSI (CET) also plays an important role in coping with fluctuating light by regulating electron transport and trans-thylakoid proton motive force (pmf) (Nakano et al., 2019; Strand et al., 2017; Wang et al., 2015), thereby inducing qE in PSII, photosynthesis control in the cytochrome (Cyt) b6/f complex and, most importantly, balancing ATP/NADPH ratio (Johnson, 2011; Shikanai and Okegawa, 2008; Suorsa et al., 2012; Yamori et al., 2015). Two CET pathways have been identified in angiosperms (Shikanai, 2014): the Proton Gradient Regulation 5 and Proton Gradient Regulation-like 1 proteins-dependent pathway (PGR5/PGRL1-CET) (DalCorso et al., 2008; Hertle et al., 2013; Munekage et al., 2002; Sugimoto et al., 2013) and the NAD(P)H dehydrogenase-like complex-dependent pathway (NDH-like-CET) (Peltier et al., 2016; Yamamoto et al., 2011). The absence of PGR5/PGRL1-CET leads to a significant PSI reduction and photoinhibition under excessive light of constant intensity (DalCorso et al., 2008; Munekage et al., 2002; Suorsa et al., 2012). In contrast, the absence of NDH-like-CET has little effects on steady-state photosynthesis under constant high light intensity (Hashimoto et al., 2003; Sazanov et al., 1998). Recent studies (Kono & Terashima, 2016; Kono et al., 2014; Yamamoto and Shikanai, 2019; Yamori et al., 2016; Zhou et al., 2022) have shown that both CET pathways contribute to P700 oxidation under fluctuating light preventing PSI photoinhibition.

The mechanism for prevention of PSI photoinhibition relies on the photosynthesis control, which was for fluctuating light conditions found by Suorsa et al. (2012). The photosynthesis control is realised by decreased rate constant of reduced plastoquinone (PQH_2) oxidation at the luminal side of Cyt b6/f by light-induced acidification of lumen; the protons in lumen creates 'backpressure' for protons to be released from PQH_2 to lumen (Rumberg & Siggel, 1968; Schansker, 2022; Siggel, 1976; Tikhonov et al., 1981). The active control results in increased oxidation state of the donor side of photosystem I (PSI), which consequently prevents PSI from photodamage by reactive oxygen species (Takagi et al., 2016; Terashima et al., 1994; Tjus et al., 1998).

Tremendous knowledge of photosynthesis regulation was accumulated by close-proximity measurements of chlorophyll fluorescence (ChlF) and transmittance using pulse amplitude modulated (PAM) measuring light, exposing plants to actinic light (AL) of constant intensity and applying multiple-turnover saturation pulses (SPs) (Schreiber, 2004). The SPs enable determination of quantum yields related to function of PSII and PSI. In case of the ChlF, however, uncoupling of ChlF signal from fraction of reduced first quinone electron acceptor in PSII, Q_A^-, due to conformational changes in PSII was reported (Laisk & Oja, 2020; Magyar et al., 2018; Oja & Laisk, 2020; Schansker et al., 2011; Sipka et al., 2021; reviewed in Garab et al., 2023). Consequently, values of the quantum yields might be distorted.

Constant light or abrupt dark-to-light transitions are rare in nature where photosynthetic organisms are typically exposed to fluctuating light. To understand the plant dynamics in fluctuating light conditions, the probing actinic light can be modulated as a sinus function of varying frequency and amplitude. Such a harmonically modulated light was proposed for studying the dynamics of photosynthesis by Nedbal and Březina (2002). The early studies conducted on tobacco (*Nicotiana tabacum*) and cyanobacterium *Synechocystis sp. PCC 6803* and, later on other organisms, revealed that photosynthetic apparatus excited by harmonically oscillating irradiance responds by an information-rich periodic pattern of ChlF emission (Nedbal & Březina, 2002; Nedbal et al., 2003, 2005). The response was strongly nonlinear and could be deconvoluted into a fundamental component, which was modulated with the same frequency as the irradiance, and a small number of upper harmonic components (Nedbal & Březina, 2002; Nedbal et al., 2003). Using a mathematical model (Nedbal et al., 2005), this complex modulation of ChlF emission was interpreted as reflecting nonlinear processes, particularly photosynthetic regulation. Recently, Nedbal and Lazár (2021) further strengthened this concept by detecting the dynamics of ChlF in the green alga *Chlorella sorokiniana* in a broad range of light frequencies (1000–0.001 Hz) and supported the proposed interpretation by new mathematical models.

Further insights into the response dynamics of photosynthetic apparatus were obtained by changing the colour of the oscillating light and by measuring the response also in CO_2 assimilation rate, F_V'/F_M', the NPQ parameter and Δ820 transmission signal (Nedbal et al., 2003). The period of light modulation in this study was 60 s and

the light oscillated with two amplitudes: between 20 and 200 and between 20 and 400 µmol photons $m^{-2} s^{-1}$, conditions like in the present study.

Multiple reporter signals, namely, ChlF, I830 and P515 transmittance, were measured also in pea (*Pisum sativum*) under oscillating light with frequency range of 1 to 1/300 Hz (Lazár et al., 2022). To access the function of PSI, PSII and pmf at thylakoid membrane (TM) in the light oscillating with 1/60 Hz frequency (60 s period), the authors applied the SPs (for ChlF and I830) or a short switching off the light (for P515). The measurements of several signals with the given approach provided new insights into the regulation of photosynthetic light reactions (Lazár et al., 2022). In a recent study, mutants of *Arabidopsis thaliana* that are defective in qE and CET were first used to identify the operational frequency range of the regulatory mechanisms by applying harmonically oscillating light with frequencies ranging from 1 to 1/480 Hz (Niu et al., 2023). It was proposed that the PsbS-dependent qE component responds to periods of oscillating light over 10 s (frequency < 0.1 Hz), while the VDE-dependent qE component operates when the period is 1 min or longer (frequency < 1/60 Hz). Furthermore, it was experimentally demonstrated that the upper harmonic modulation of signals was induced by the regulatory processes of the light-dependent photosynthetic reactions (Niu et al., 2023).

In the present study, we investigated the response of different photosynthetic regulatory processes to light oscillating at a single frequency (1/60 Hz). We combined the harmonically oscillating light of various amplitudes with the SPs, which enabled calculation of the quantum yields and fractions of reduced (oxidised) forms of electron carriers. The frequency of 1/60 Hz was selected because it is characteristic for the spontaneous oscillations occurring in plants (Ferimazova et al., 2002; Lazár et al., 2005) and corresponds to a photosynthetic resonance that was identified in Nedbal and Březina (2002), Lazár et al. (2022) and Niu et al. (2023). The light oscillated with three different amplitudes, covering the range from light limitation to saturation. The interpretation of the results was strengthened by measuring simultaneously multiple variables (ChlF, redox changes of plastocyanin, P700 and ferredoxin) and comparing the dynamics in wild-type plants of *A. thaliana* with mutants. The dynamics of qE-related regulatory processes were studied in the *npq1* mutant (Niyogi et al., 1998) lacking VDE-dependent qE component and the *npq4* mutant (Li et al., 2000) lacking PsbS-dependent qE component. The operation of CET pathways was inspected in the *crr2-2* mutant (Hashimoto et al., 2003) that is incompetent in the NDH-like-CET pathway, and the *pgrl1ab* mutant (DalCorso et al., 2008) that is defective in the PGR5/PGRL1-CET pathway.

2 | MATERIALS AND METHODS

2.1 | Plant materials and growth conditions

Six genotypes of *A. thaliana* plants, including wild-type Col-0 (Columbia-0, the background of *npq1*, *npq4* and *pgrl1ab*), wild-type Col-*gl1* (trichome-lacking *glabrous 1*, the background of *crr2-2*), *npq1* (VDE-deficient), *npq4* (PsbS-deficient), *pgrl1ab* (lacking the PGR5/PGRL1-dependent pathway of CET) and *crr2-2* (lacking the NDH-like complex-dependent pathway of CET) were grown under controlled climate conditions. All seeds were first sown in commercial substrate (Pikier, Balster Einheitserdewerk). After 3 days of stratification in a dark room at 4°C, sowing panels were moved to a climate chamber at a photoperiod of 12 h/12 h light/dark, a day/night temperature of 26°C/20°C and a constant relative air humidity of 60%. The photosynthetic photon flux density (PPFD) of growth light (Fluora L 58 W/77; Osram) was approximately 100 µmol photons $m^{-2} s^{-1}$. Two weeks after sowing, the seedlings were transplanted into pots (7 × 7 × 8 cm, one plant per pot) filled with commercial substrate (Lignostrat Dachgarten extensiv; HAWITA). Plants were watered from the bottom to maintain soil moisture. Measurements were started on the 36th day after sowing; by this time, mature leaves were large enough to cover the entire measurement area of the DUAL-KLAS-NIR instrument (see below).

2.2 | Instrument setting of chlorophyll fluorescence and KLAS-NIR measurements

The DUAL-KLAS-NIR spectrophotometer (Heinz Walz GmbH) with a 3010-DUAL leaf cuvette was used for monitoring the ChlF yield and relative redox changes of the primary donor of PSI (P700), plastocyanin (PC) and ferredoxin (Fd) simultaneously. The KLAS-100 software (Heinz Walz GmbH) was used to implement the measurement and record the data. The red light (630 nm) was applied from both sides of the leaf as AL. The pulse-amplitude-modulated green light (540 nm, 6 µmol photons $m^{-2} s^{-1}$) was applied from the abaxial side of the leaf as measuring light (ML) of ChlF yield. In parallel with the ChlF detection, four dual-wavelength difference transmittance signals in near-infrared (780–820, 820–870, 870–965 and 840–965 nm wavelength pairs; NIR-ML) were measured and deconvoluted into relative redox changes of P700, PC and Fd. The deconvolution depends on the selective differential transmission spectra of P700, PC and Fd at these four wavelength pairs, called 'differential model plots', which were determined a priori on overnight dark-adapted plants following the default procedures provided by the KLAS-100 software (Klughammer & Schreiber, 2016). Specific differential model plots were determined for each genotype and used for subsequent measurements for all plants of the same genotype grown under the same environments.

2.3 | Light response curve measurement

Overnight dark-adapted plants were taken out of the climate chamber at the end of the dark period of the day/night regime and kept in the darkness until the measurements began in the laboratory. The maximum oxidation of P700 (P_m) and PC (PC_m) and the maximum reduction of Fd (Fd^-_m) were determined for each dark-adapted plant

by performing the NIR-MAX routine before starting the measurements (Klughammer & Schreiber, 2016). Subsequently, the rapid light response curve was measured for each plant by increasing the AL intensity in eight steps: 67, 99, 133, 182, 247, 425, 671 and 1049 µmol photons $m^{-2} s^{-1}$. The light remained constant at each intensity for 60 s (the instrument predefined protocol). The first multiple-turnover SP (630 nm, 300 ms duration, 3700 µmol photons $m^{-2} s^{-1}$) was given in the dark to determine the maximum yield of ChlF, F_m, to estimate the maximum quantum yield of PSII photochemistry. After a 40-s delay, the AL was switched on and increased in eight steps as described above. High-intensity SP (630 nm, 300 ms duration, 17 000 µmol photons $m^{-2} s^{-1}$) was given at the end of each light step to estimate the quantum yields of PSI and PSII (see Lazár et al., 2022) and the apparent relative oxidation/reduction of PC and Fd. Three to seven plants were measured as biological replicates of each genotype.

2.4 | Harmonically oscillating light measurement with saturation pulse analysis

The NIR-MAX routine was performed for each plant as described above to determine the P_m, PC_m and Fd^-_m before measurements. After that, the measurement combining harmonically oscillating light with SPs was conducted. The first SP (630 nm, 300 ms duration, 3700 µmol photons $m^{-2} s^{-1}$) was given in the dark to determine the F_m. Then, with a 25-s delay, the oscillating AL with 1/60 Hz (= period of 60 s) was triggered and continued for 40 cycles. The first 10 cycles were applied without SPs to establish a stationary dynamic pattern and to allow the dark-adapted leaf to adapt to light. During these 10 cycles, the four dynamic signals (PSII ChlF and relative redox changes of PSI, PC and Fd) were recorded under oscillating light without any interference from SPs. Starting from the 11th cycle, a high-intensity SP (630 nm, 300 ms duration, 17 000 µmol photons $m^{-2} s^{-1}$) was triggered during each cycle (one SP per cycle) at different phases of AL oscillation to cover the entire period of oscillation within 30 cycles (Supporting Information S1: Figure SM1A). Therefore, the maximum ChlF yield (F_m') at different phase of AL oscillation, as well as the maximum oxidation of P700, PC (P_m', PC_m') and maximum reduction of Fd (Fd^-_m') can be quantified. For detailed descriptions of the combined measurement of photosynthetic efficiency under oscillating light, see (Lazár et al., 2022). Three different amplitudes of AL oscillation were implemented, covering different light ranges on the light response curves: 100–200, 100–400 and 100–800 µmol photons $m^{-2} s^{-1}$. Due to the limitations of the DUAL-KLAS-NIR instrument to adjust the light intensity levels, the oscillating AL was modulated incrementally rather than smoothly. A comparison of the real light modulation with the expected light modulation is shown in Supporting Information S1: Figure SM1B. Three to seven plants were measured as biological replicates for each genotype in each amplitude of oscillation. Based on the values of ChlF and dual-wavelength difference transmittance signals measured in the dark-adapted state with and without the SP, and in the light-adapted state with the SP and just before application of the SP, quantum yields of PSI and PSII and apparent relative redox states of PC and Fd were estimated (Lazár et al., 2022; Schreiber & Klughammer, 2016).

3 | RESULTS

3.1 | Rapid light response curves

The experiments started with measuring the rapid light response curves with 60 s dwell time at each light intensity step (Figure 1). The light intensities used were from the ranges of light oscillations in the second part of the experiments, as indicated by the arrows in Figure 1c. The rapid light response curves show that the low-amplitude oscillations (LL) were varying largely in the linear part of the rapid light response curves whereas the high-amplitude oscillations (HL) reached, at their maxima, into the saturation range of all probed signals.

The graphs represent (by different colours) data of wild types (Col-0 and Col-*gl1*), *npq* mutants (*npq1*, *npq4*) and CET mutants (*crr2-2*, *pgrl1ab*) of *A. thaliana*. The transmittance measurements were used to determine PSI quantum yields: the effective photochemical quantum yield of PSI, Y(I) in Figure 1a; the quantum yield of nonphotochemical energy dissipation in PSI due to donor side limitation, Y(ND) in Figure 1b; and the quantum yield of nonphotochemical energy dissipation in PSI due to acceptor side limitation, Y(NA) in Figure 1c. The PSII-related parameters were calculated from the ChlF measurements: the effective photochemical quantum yield of PSII, Y(II) in Figure 1d; the quantum yield of the regulated nonphotochemical quenching in PSII, Y(NPQ) in Figure 1e; and the quantum yield of the constitutive (always present) nonphotochemical quenching in PSII, Y(NO) in Figure 1f. The coefficient of photochemical quenching qP in Figure 1g was also evaluated from the ChlF measurements and served further as a proxy for the fraction of open PSII centres (with Q_A oxidised). This interpretation of qP is based on the model of energetically separated PSII units (reviewed in Stirbet, 2013); existence of energetic connectivity among PSIIs was recently ruled out (Oja & Laisk, 2020). The apparent relative oxidation of PC (PC Ox) and apparent relative reduction of Fd (Fd Red) shown in Figure 1h,i were also estimated from transmittance measurements.

Before describing the results, we want to make a note on the PSII quantum yields determined from ChlF measurements by means of application of the SPs. According to the original hypothesis of Duysens and Sweers (1963), which is the theoretical basis behind the evaluation of the PSII quantum yields, the higher the fraction of Q_A^- is, the higher the ChlF emission will be. However, as outlined in the introduction, changes in ChlF might occur without changes of the redox state of Q_A. In detail, if a multiple turnover SP is applied, the ChlF rises during the pulse even if Q_A is reduced in the initial part of the pulse (a similar result is obtained with a series of single turnover saturating flashes). Therefore, the F_M and F_M's might be overestimated, which affects values of the PSII quantum yields (overestimated Y(II) and

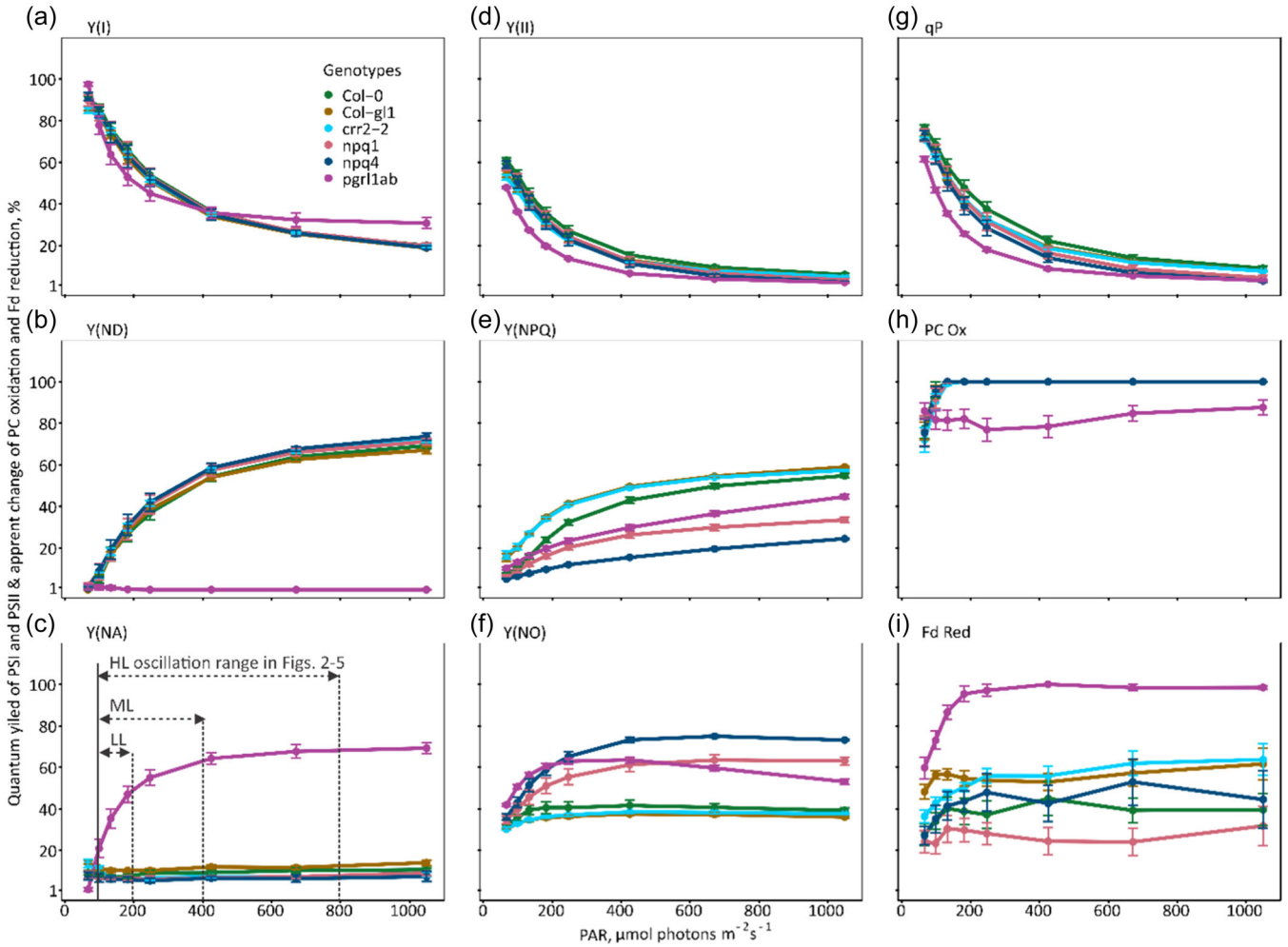

FIGURE 1 The quantum yields of photosystems and redox states of electron carriers were evaluated in rapid light response curves with six genotypes of *Arabidopsis thaliana*: Col-0, Col-*gl1*, *npq1*, *npq4*, *crr2-2* and *pgrl1ab* (see legend in panel (a)). The quantum yields of photosystem I and hotosystem II functions are shown from panels (a) to (f), the apparent oxidation/reduction changes of plastocyanin (PC Ox) and ferredoxin (Fd Red) are shown in panels (h) and (i), and panel (g) shows changes of qP. The error bars represent the standard error (n = 3–7). The horizontal dashed arrows in panel (c) indicate the ranges of light intensity oscillation that were used in further experiments: low-light oscillations (LL, 100–200 µmol photons m^{-2} s^{-1}), medium-light oscillations (ML, 100–400 µmol photons m^{-2} s^{-1}) and high-light oscillations (HL, 100–800 µmol photons m^{-2} s^{-1}). qP, the coefficient of photochemical quenching.

underestimated of Y(NO) and Y(NPQ)). Nevertheless, as discussed by Oja and Laisk (2020), under natural light intensities, the quantum yield of photosynthesis is indeed more or less proportional to the efficient quantum yield of PSII photochemistry determined by means of the SP-PAM measurement of ChlF. In the case of the oscillating actinic light, we showed (Lazár et al., 2022) that values of the PSII quantum yields corrected for potentially overestimated F_M's are indeed changed but resulted values of the yields follow the same trends during oscillating actinic light period as values of the yields calculated on the basis of uncorrected values of F_M's. In this work, we assume (no data exist against the assumption) that the potential overestimation of F_M's is the same for all *A. thaliana* genotypes (wild types and all mutants). Hence, since we are interested in changes (not values) of the yields during the oscillating actinic light, the correction for potentially overestimated F_M's would not affect a conclusion, and therefore, we do not perform any correction of F_M's in this work.

The rapid light response curves were different for different reporter signals. On the extremes, Fd reduction state and PC oxidation state were increasing with the constant light only below 200 µmol photons m^{-2} s^{-1}, whereas the yields of Y(I), Y(II), Y (NPQ) reached stationary levels in all tested genotypes only above 500 µmol photons m^{-2} s^{-1}. The curves representing quantum yields related to the PSI function, Y(I), Y(NA) and Y(ND) (Figure 1a–c) were similar across all genotypes except for the *pgrl1ab*. When PAR rose from low levels, Y(NA) of all genotypes (Figure 1c), except *pgrl1ab*, decreased rapidly as downstream reactions at the PSI acceptor side were activated by light, and Y (ND) was subsequently enhanced (Figure 1b). In the *pgrl1ab*

mutant, however, the Y(NA) largely increased with rising light intensity while Y(ND) stayed low at all light intensities.

The dynamics of Y(NA) and Y(ND) were consistent with the redox states of Fd at the acceptor side of PSI and PC at its donor side. In the Col-0, PC rapidly reached a fully oxidised state at AL intensity of about 200 µmol photons m^{-2} s^{-1} and higher (Figure 1h), while Fd was partially reduced with increasing light and then remained relatively stable (Figure 1i). In contrast, *pgrl1ab* showed a substantially higher reduction level of Fd (Figure 1i) and a decreased level of PC oxidation (i.e. higher PC reduction) than Col-0 (Figure 1h). The electron congestions at the acceptor side of PSI appeared to limit the efficiency of electron transport throughout the entire electron transport chain in *pgrl1ab*, as indicated by the lower fraction of the open PSII reaction centres (proxied by qP) in this mutant (Figure 1g). The changes in Y(I), Y(NA) and Y(ND) in the other CET mutant, *crr2-2*, were identical to its wild-type Col-*gl1* in constant light illumination (Figure 1a–c) except at the low light intensities in which Fd was less reduced in *crr2-2* than in Col-*gl1* (Figure 1i). The *npq1* and *npq4* mutants were largely comparable with Col-0 in the PSI-related quantum yields (Figure 1a–c) and the redox changes of PC and Fd (Figure 1h,i), although Fd tended to stay more oxidised in *npq1* than the others.

Y(II) was generally comparable among the genotypes, with a slightly lower value in the *prgl1ab* mutant (Figure 1d). Y(NPQ) of both *npq1* and *npq4* was considerably lower than that of Col-0 (Figure 1e) due to the qE deficiency (Li et al., 2000; Niyogi et al., 1998); since the PsbS- and VDE-dependent mechanisms are activated independently (Holzwarth et al., 2006; Li et al., 2000), a residual qE was present in particular mutants. The lower level of Y(NPQ) in the *npq1* and *npq4* was compensated by a higher level of Y(NO) (Figure 1f), resulting in the same sum of Y(NPQ) and Y(NO) for the *npq* mutants and Col-0 (since Y(II) + Y(NPQ) + Y(NO) = 1). The *pgrl1ab* mutant also had lower Y(NPQ) than Col-0 (Figure 1e), consistent with the role of the PGR5/PGRL1-CET in lumen acidification and thus the qE induction (DalCorso et al., 2008; Munekage et al., 2002). The effects of lacking different protective mechanisms on the induction of qE can also be visualised by the commonly used NPQ parameter, which equals to Y(NPQ)/Y(NO), (reviewed in Lazár, 2015). Therefore, changes in the NPQ parameter (Supporting Information S1: Figure SM2A) can be expected based on the values of Y(NPQ) and Y(NO) shown in Figures 1e, f. Contrary to *pgrl1ab*, Y(NPQ) and NPQ parameter of the *crr2-2* mutant was the same as that of Col-*gl1*, supporting the notion that the NDH-like-CET may not be essential for the regulation of qE and electron transport in relatively constant excess light conditions (Hashimoto et al., 2003). However, we cannot rule out the possibility that a lack of NDH-like CET was (partly) compensated by PGR5/PGRL1 CET as was found in measurements with PGR5/PGRL1 and NDH-like CET double mutants (Nakano et al., 2019).

The Y(I)–Y(II) parameter (Huang et al., 2011; Miyake et al., 2005; Sagun et al., 2019; Yamori et al., 2011) (Supporting Information S1: Figure SM2B) was used to estimate the quantum yield of CET. The Y(I)/Y(II) parameter (Kono et al., 2014; Miyake et al., 2005; Yamori et al., 2011) (Supporting Information S1: -Figure SM2C) represents the relative quantum yield of CET. While Y(I)/Y(II) showed a seeming advantage for discriminating differences among the genotypes, it is important to keep in mind that a high value of Y(I)/Y(II) might simply be caused by unchanged Y(I) with Y(II) approaching zero, as is the case in the *pgrl1ab*, *npq1* and *npq4* mutants (cf. Figure 1a,d and Supporting Information S1: -Figure SM2C). Notably, the absence of the PGR5/PGRL1-CET did not result in a low level of Y(I)–Y(II) or Y(I)/Y(II), as the *pgrl1ab* mutant showed high levels of both parameters (Supporting Information S1: Figure SM2B,C). The potentially overestimated F_M' values (see above) might even underestimate values of Y(I)–Y(II) and Y(I)/Y(II). We further note that unspecified effects caused by mutations other than those related to the PGRL1A and PGRL1B proteins, as was found for the *pgr5-1* mutant (Wada et al., 2021), can be ruled out in the *pgrl1ab* mutant, since the $pgr5^{hope1}$ mutant lacking only the PGR5 protein has the same phenotype as *pgrl1ab* mutant (Wada et al., 2021).

In summary, the *pgrl1ab*, *npq1* and *npq4* mutants showed altered phenotypes compared to their wild-type Col-0 when exposed to AL of 60 s constant intensity during the light response curve measurements, whereas the *crr2-2* mutant was largely indistinguishable from its wild-type Col-*gl1*. These results confirm the previously described phenotypes of these mutants (DalCorso et al., 2008; Hashimoto et al., 2003; Li et al., 2000; Niyogi et al., 1998).

3.2 | Saturation pulse analysis under light oscillating with frequency of 1/60 Hz (period of 60 s)

Three different amplitudes, low-light (LL, 100–200 µmol photons m^{-2} s^{-1}), medium-light (ML, 100–400 µmol photons m^{-2} s^{-1}) and high-light oscillations (HL, 100–800 µmol photons m^{-2} s^{-1}) were applied to study plant dynamics reaching from light-limited to light-saturated levels (Figure 1, Supporting Information S1: -Figure SM1B). A single frequency of 1/60 s^{-1} of the light modulation was applied in this study (other frequencies were explored in Niu et al., 2023). The quantum yields and redox states were probed by SPs of light, one pulse per period, that were given on top of the AL oscillations, always slightly phase-shifted. In this way, the dynamics of the measured signals were probed with a minimal disruption along the entire period (see Section 2 and Supporting Information S1: Figure SM1A).

The results are presented in Figures 2–5 in a condensed way where the response to individual SP is plotted relative to the phase of the light oscillation at which the pulse was applied. Namely, the phases 0° and 360° represent SPs that were applied at the minimum of the light oscillation, 60 s apart. The phase 180° represents an SP that was given at the maximum of the light period, 30 s from the light minima. Circles, triangles and squares represent the LL, ML and HL oscillations, respectively. Different

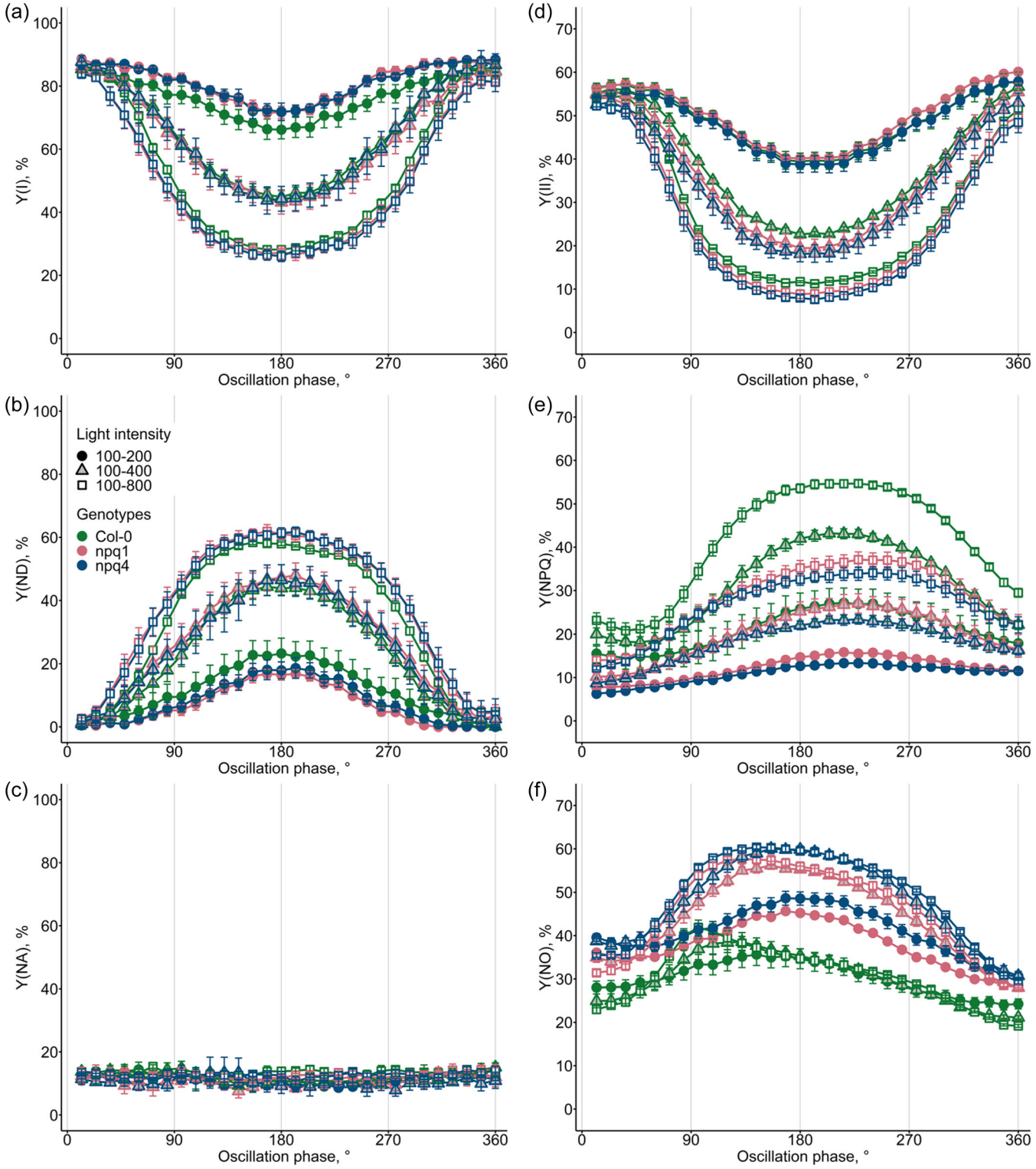

FIGURE 2 Changes in photosystem I- (a - c) and photosystem II-related (d - f) quantum yields of the three qE-related genotypes of *Arabidopsis thaliana*, Col-0, *npq1* and *npq4*, under three different amplitudes of oscillating light ranging from 100 to 200 µmol photons m^{-2} s^{-1}, 100 to 400 µmol photons m^{-2} s^{-1} and 100 to 800 µmol photons m^{-2} s^{-1}. The error bars represent the standard error (n = 3–7). qE, energy-dependent nonphotochemical quenching. [Color figure can be viewed at wileyonlinelibrary.com]

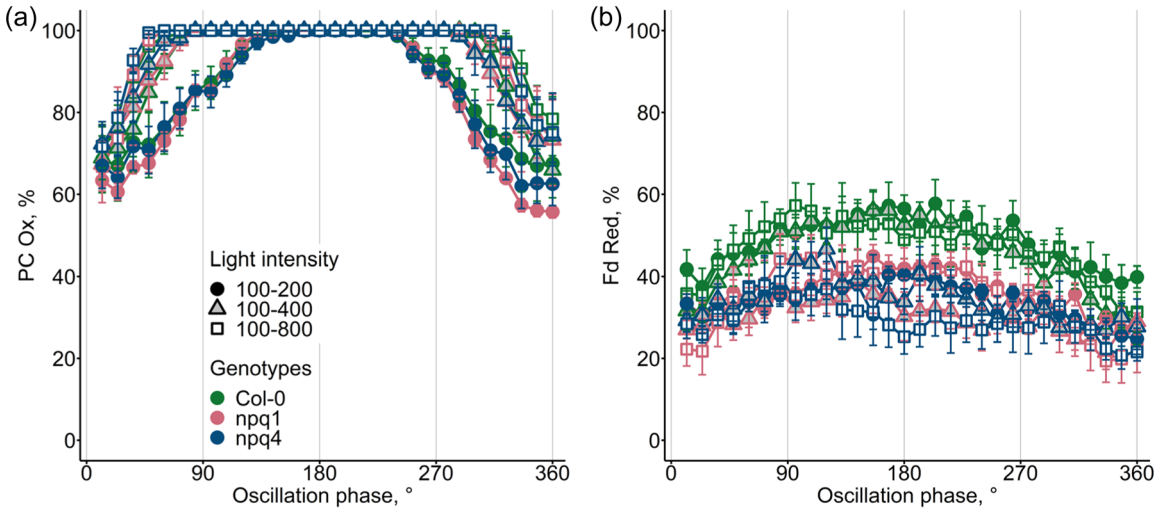

FIGURE 3 Changes of the apparent relative oxidation of plastocyanin (PC Ox, a) and reduction of ferredoxin (Fd Red, b) in response to three different amplitudes of oscillating light for the three qE-related genotypes of *Arabidopsis thaliana*, Col-0, *npq1* and *npq4*. The oscillating light amplitudes range from 100 to 200 µmol photons m^{-2} s^{-1}, from 100 to 400 µmol photons m^{-2} s^{-1} and from 100 to 800 µmol photons m^{-2} s^{-1}. The error bars represent the standard error (n = 3–7). qE, energy-dependent nonphotochemical quenching. [Color figure can be viewed at wileyonlinelibrary.com]

colours denote plant genotypes, as explained in legends placed in one of the figure panels.

3.2.1 | The Col-0 wild type and *npq* mutants

The oscillating light-induced modulations in the PSI- and PSII-related quantum yields were generally small in LL oscillation but became larger as the light oscillating amplitudes increases (with the exception of Y(NA), Figure 2c). Notably, the changes in Y(I) (Figure 2a), Y(II) (Figure 2d) and Y(ND) (Figure 2b) show nearly symmetrical patterns closely mirroring the light modulation. The minimum of Y(I) and Y (II) and the maximum of Y(ND) coincided with maximum of light oscillations (phase 180°). A contrasting response to the light oscillations was found with Y(NA) in Figure 2c, which remained below 20% across all genotypes and light intensities, essentially unaffected by the light oscillations. The trend of Y(ND) (Figure 2b) complements that of Y(I) (Figure 2a). These phenomena held true for the wild-type Col-0 and both *npq* mutants.

Another contrasting dynamic response was found with Y(NPQ) in Figure 2e. The minima and maxima of Y(NPQ) were delayed by approximately 45° (7.5 s) relative to the course of HL oscillation, reflecting the time necessary to activate and deactivate the regulatory qE. The strength of the regulatory response was increasing with amplitude of the light and was, understandably, stronger in the Col-0 wild type (green lines and symbols) compared to the qE-impaired mutants *npq1* (pink lines and symbols) and *npq4* (dark blue lines and symbols). The qE response was weaker in *npq4* than in *npq1*.

The weak Y(NPQ) responses in the *npq* mutants were compensated by increased levels and modulation of the quantum yield of the constitutive nonphotochemical quenching in PSII, Y(NO) in Figure 2f. As a result, the sum of Y(NPQ) and Y(NO) was about the same for Col-0 and the *npq* mutants for the given range of the sinusoidal illumination, as deduced from roughly the same magnitudes of Y(II) (Figure 2d) in all three (with slightly lower values in the mutants compared to Col-0 in ML and HL oscillations) and considering that Y (II) + Y(NPQ) + Y(NO) = 1. Interestingly, the strongest response of Y (NO) in the Col-0 wild type (green, Figure 2f) during the rising phase of the light oscillation, between 90° and 180°, again compensated for the delayed Y(NPQ) (green, Figure 2e). This qualitative pattern was also found in both mutants with HL (squares) and ML oscillations (triangles). The low-light oscillations (circles) were not strong enough to elicit similar response in the mutants.

It should be noted that the NPQ parameter (= Y(NPQ)/Y(NO)) of both *npq1* and *npq4* displayed roughly monotonically increasing trends in all oscillating light amplitudes (Supporting Information S1: Figure SM3A). However, it is premature to draw the conclusion that qE of both mutants does not respond to oscillating light illumination based solely on this parameter. Such a conclusion is not supported by the courses of Y(NPQ) and Y(NO) (Figure 2e,f).

Generally, in comparison to wild-type Col-0, the *npq1* and *npq4* mutants displayed little difference in their responses concerning PSI-related quantum yields, Y(I), Y(ND) and Y(NA) (Figure 2a–c). This implies that the defects in qE had barely any impact on PSI functionality, encompassing both its donor and acceptor sides. Regarding PSII-related quantum yields, while an apparent reduction of Y(NPQ) was shown in mutants (Figure 2e), the trend in Y(II) (Figure 2d) was similar between the *npq* mutants and wild-type Col-0. Minor difference occurred primarily in the ML and HL oscillations (Figure 2d), where the mutants displayed slightly lower Y(II) than wild-type Col-0, with *npq4* exhibiting lower

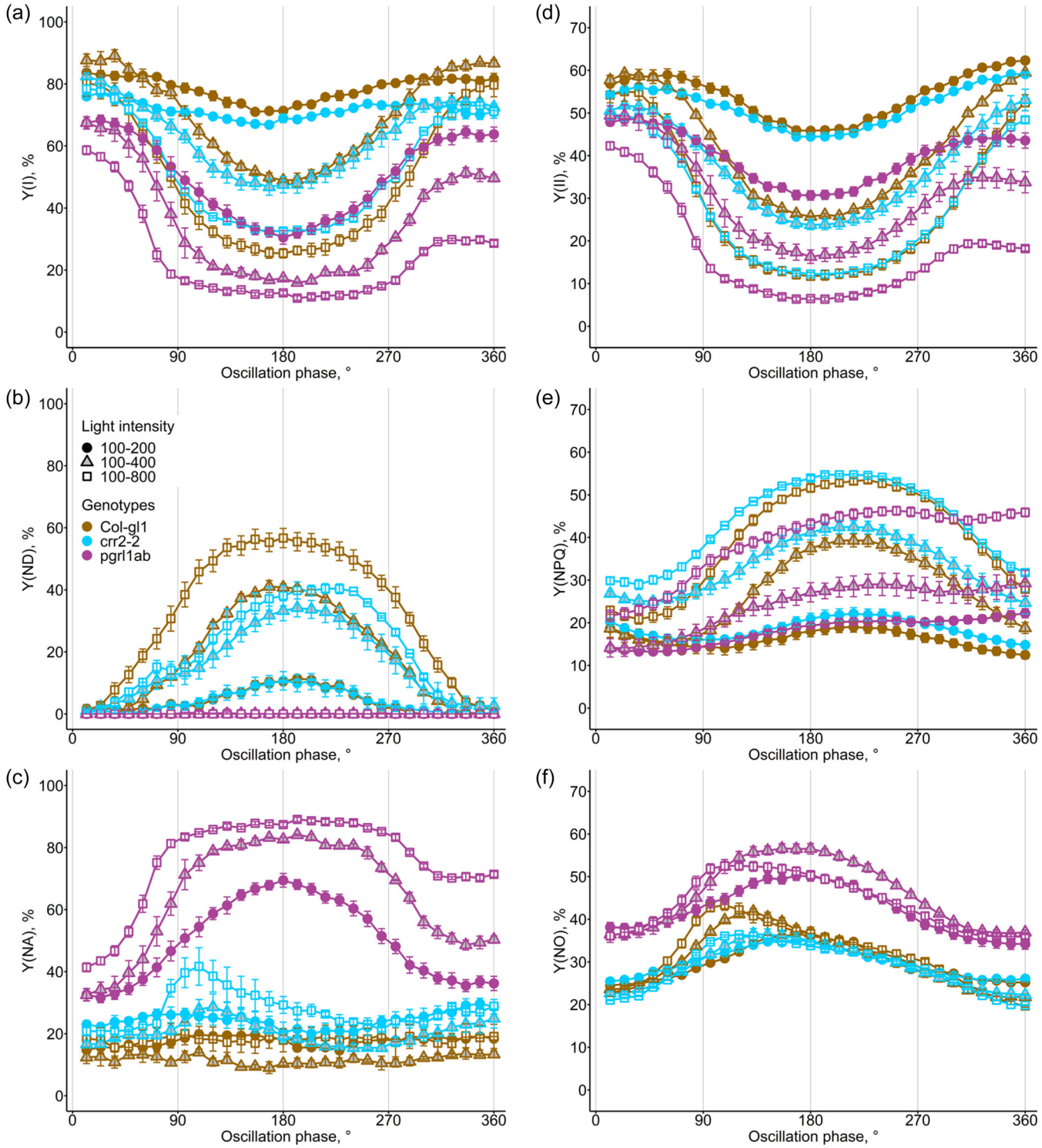

FIGURE 4 Changes in photosystem I- (a-c) and photosystem II-related (d-f) quantum yields of the three CET-related genotypes of *Arabidopsis thaliana*, Col-*gl1*, *crr2-2* and *pgrl1ab*, under three different amplitudes of oscillating light ranging from 100 to 200 µmol photons m^{-2} s^{-1}, from 100 to 400 µmol photons m^{-2} s^{-1} and from 100 to 800 µmol photons m^{-2} s^{-1}. The error bars represent the standard error (n = 3–7). CET, cyclic electron transport. [Color figure can be viewed at wileyonlinelibrary.com]

values than *npq1*. This suggests that the ability of the *npq* mutants to maintain PSII efficiency under oscillating light illumination was slightly restricted compared to their wild-type Col-0, with the *npq4* performing worse than the *npq1* (Figure 2d).

For the *npq* mutants and their corresponding wild-type Col-0, the oxidation process of PC under LL oscillation (cycles, Figure 3a) closely followed the course of the light intensity changes, but stayed at the maximal oxidation even before and following the maximum of the

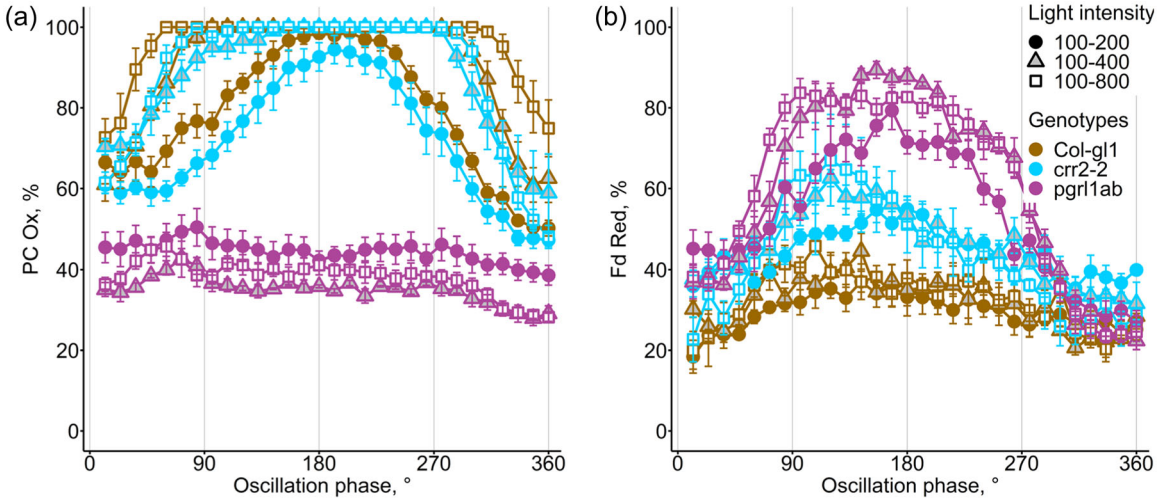

FIGURE 5 Changes of the apparent relative oxidation of plastocyanin (PC Ox, a) and reduction of ferredoxin (Fd Red, b) in response to three different amplitudes of oscillating light for the three CET-related genotypes of *Arabidopsis thaliana*, Col-*gl1*, *crr2-2* and *pgrl1ab*. The oscillating light amplitudes range from 100 to 200 µmol photons m^{-2} s^{-1}, from 100 to 400 µmol photons m^{-2} s^{-1} and from 100 to 800 µmol photons m^{-2} s^{-1}. The error bars represent the standard error (n = 3–7). CET, cyclic electron transport. [Color figure can be viewed at wileyonlinelibrary.com]

oscillating light intensity (spanning phases approximately from 135° to 225°). Under ML and HL oscillations (triangles and squares, Figure 3a), the saturation of PC oxidation was more pronounced, maintaining maximum oxidation between phases approximately from 90° to 270°. In contrast, the redox state of Fd exhibited limited alignment with light oscillations, irrespective of the genotype or light oscillation amplitude (Figure 3b). Notably, *npq4* and *npq1* consistently exhibited lower levels of Fd reduction compared to Col-0 across all oscillating light amplitudes.

In addition, the impact of the qE deficiency on CET in oscillating light was elucidated in Supporting Information S1: Figure SM3. Both *npq* mutants had elevated quantum yields of CET, Y(I)-Y(II), in comparison to Col-0 under LL and ML oscillations, but showed similar levels as Col-0 under HL oscillations (Supporting Information S1: Figure SM3B). A more dramatic contrast appeared in the relative quantum yields of CET, Y(I)/Y(II), which followed the course of light oscillations with more substantial modulations in HL oscillation and fewer changes in LL oscillation (Supporting Information S1: -Figure SM3C). Both *npq* mutants exhibited higher Y(I)/Y(II) than Col-0, with the *npq4* showing the highest values. These results suggest that a potential enhancement of CET might occur in *npq* mutants as a mechanism to alleviate the pressure on electron transport chain under oscillating light conditions. This may partly explain the less reduction of Fd in *npq* mutants than in Col-0 (Figure 3b).

3.2.2 | The CET mutants

The wild-type Col-*gl1* (background of *crr2-2*) behaved in much the same way as the wild-type Col-0 (background of *pgrl1ab*) in terms of the dynamics of all tested photosynthetic parameters under light oscillations (cf. green symbols and lines in Figure 2 and gold symbols and lines in Figure 4).

Regarding the changes in Y(I) and Y(II) of *crr2-2* in oscillating light, they were roughly similar to those of Col-*gl1*, with some differences (light blue and gold symbols and lines, Figure 4a,d). Both Y(I) and Y(II) were slightly lower in *crr2-2* than in Col-*gl1* under LL oscillation. Under ML oscillations, *crr2-2* showed constrained recovery of Y(I) and Y(II) as the light approached the lowest intensity, particularly around phases 0°–60° and 300°–360°. During HL oscillation, Y(I) (Figure 4a), but not Y(II) (Figure 4d) in *crr2-2* was higher than in Col-*gl1* around the maximum intensity of oscillating light. The most distinctive feature of the *crr2-2* mutant, in contrast to Col-*gl1*, was its smaller donor side limitation of PSI (Y(ND), Figure 4b) but higher acceptor side limitation of PSI (Y(NA), Figure 4c) under ML and HL oscillations. This contrast was especially evident during the ascending phase of HL oscillation, where Y(NA) of *crr2-2* exhibited a peak at approximately 90° phase (squares with light blue in Figure 4c) accompanied by a shallow depression phase of Y(ND) (Figure 4b). These results suggest that the absence of NDH-like-CET might diminish the capacity of the PSI acceptor side to relieve electron pressure in the initial rising phase of HL oscillation.

The *pgrl1ab* mutant had significantly lower photochemical efficiencies of both PSI and PSII (magenta symbols and lines in Figure 4a,d) when compared to Col-0 (green symbols and lines in Figure 2a,d) and the other plants, regardless of the oscillation amplitude. Under all oscillation amplitudes, this mutant consistently displayed notably higher Y(NA) (Figure 4c), while Y(ND) was entirely absent (Figure 4b). These data highlight the essential role of PGR5/PGRL1-CET in facilitating electron release at the PSI acceptor side

and oxidation at the PSI donor side under oscillating light, regardless of the amplitude.

Notably, mutants with CET defects exhibited variations in their NPQ-related parameters compared to their respective wild types, with two mutants showing entirely distinct behaviours. The *crr2-2* mutant had the same course and slightly higher values of Y(NPQ) as Col-*gl1* under LL oscillations, with notably higher values at the beginning and end phases of the oscillation period under ML and HL oscillations (Figure 4e). Conversely, in comparison to Col-0 (green, Figure 2e), Y(NPQ) of the *pgrl1ab* mutant (magenta, Figure 4e) was lower at the beginning but higher at the end phase of the oscillation period, indicating that the course of Y(NPQ) in *pgrl1ab* did not follow the course of the oscillating light intensity. Apparent differences between CET mutants and their respective wild types were also able to be observed in the NPQ parameter (Supporting Information S1: Figures SM4A and SM3A). The NPQ parameter in *crr2-2* followed a similar pattern to Col-*gl1* but with remarkably higher values in all amplitudes of light oscillation (Supporting Information S1: -Figure SM4A). Conversely, values of NPQ parameter of *pgrl1ab* were much lower (Supporting Information S1: Figure SM4A) than those of Col-0 and followed the same courses as seen in both *npq1* and *npq4* mutants in all oscillation amplitudes (Supporting Information S1: -Figure SM3A). The delay in Y(NPQ) minima and maxima relative to light oscillations, previously observed in Col-0 wild type and *npq* mutants (Figure 2e), was also present in the *crr2-2* mutant and Col-*gl1* wild type (approximately 45° phase delay relative to the course of HL oscillation, 7.5 s) (Figure 4e). In the case of NPQ parameter, a similar delay was observed in *crr2-2* and Col-*gl1* (Supporting Information S1: Figure SM4A), but it was more pronounced to approximately 90° (15 s) phase delay relative to the course of HL oscillation. In the *pgrl1ab* mutant (Figure 4e), there was still an observable delay of Y(NPQ), but it was highly overshadowed by the overall upward trend.

In Col-*gl1* and both CET mutants, the courses of Y(NO) aligned with the changes of light intensity in LL oscillation (Figure 4f). However, this alignment was substantially distorted in ML and HL oscillations of Col-*gl1*, as well as in HL oscillation of both mutants. The delayed responses of Y(NPQ) (Figure 4e) seem to be partially compensated by the increased levels and modulation of Y(NO) (Figure 4f). For LL oscillation, Y(NO) of *crr2-2* closely resembled that of Col-*gl1* (Figure 4f), whereas Y(NO) of *pgrl1ab* was much higher than that of Col-0 (Figure 2f). For ML and HL oscillations, Y(NO) of *crr2-2* was lower than Y(NO) of Col-*gl1* in the raising phase of light oscillation, whereas Y(NO) of *pgrl1ab* remained well above Y(NO) of Col-0 (Figures 2f and 4f). Similar to the *npq* mutants (Figure 2e,f), the consistently enhanced Y(NO) in *pgrl1ab* may act to partially compensate the lower Y(NPQ) (Figure 4e,f). Considering again that Y(II) + Y(NPQ) + Y(NO) = 1, the sum of Y(NPQ) and Y(NO) was slightly higher for *crr2-2*, but considerably higher for *pgrl1ab* than in their respective wild types (Figures 2d and 4d).

The PC oxidation in *crr2-2* was smaller than in Col-*gl1* during LL oscillation, and smaller at the beginning and the end phases of oscillation in ML and HL oscillations (Figure 5a). Regarding the PSI acceptor side, Fd (Figure 5b) in *crr2-2* was more reduced than in Col-*gl1*, especially evident in ML and HL oscillations where a peak can be observed in *crr2-2* at roughly 90° phase. The lower oxidation of PC (Figure 5a) and higher reduction of Fd in *crr2-2* (Figure 5b) compared to Col-*gl1* were consistent with a smaller Y(ND) (Figure 4b) and a larger Y(NA) (Figure 4c) in this mutant, further confirming that the absence of NDH-like-CET caused PSI acceptor side limitation, particularly in ML and HL oscillations.

On both the PSI donor and acceptor sides, the *pgrl1ab* mutant (Figure 5) had dramatic differences from its wild-type Col-0 (Figure 3). The mutant exhibited markedly higher Fd reduction (Figure 5b) and consistently low and relatively stable PC oxidation (Figure 5a), irrespective of the amplitude of the oscillating light. These findings were in line with the strong Y(NA) (Figure 4c) but zero Y(ND) (Figure 4b) observed in *pgrl1ab* and provided further indication that electron congestion occurred in the PSI acceptor side of *pgrl1ab* in all intensities of oscillating light.

An intriguing phenomenon occurred in *pgrl1ab* was that certain parameters showed different values at the beginning and end of the oscillation period, namely, Y(I), Y(NA), Y(II), Y(NPQ) (Figure 4a,c–e) and Fd reduction (Figure 5b). The lower values of Y(II) and Y(I) at the end than at the beginning of the light oscillation period were counter-balanced by higher values of Y(NPQ) and Y(NA), respectively. This was consistently observed in *pgrl1ab* and was more pronounced in HL than in ML oscillations. Given that this behaviour occurred only in the *pgrl1ab* mutant, it reflects its functional characteristics rather than measurement errors.

In terms of the quantum yield of the CET (Supporting Information S1: Figure SM4B), Y(I)-Y(II) in *crr2-2* was lower in LL oscillations but higher in HL oscillations when compared to Col-*gl1*. For the relative quantum yield of the CET, Y(I)/Y(II), *crr2-2* also displayed higher values than Col-*gl1* under HL oscillations (Supporting Information S1: Figure SM4C). In contrast, for *pgrl1ab* mutant, both Y(I)-Y(II) (Supporting Information S1: Figure SM4B) and Y(I)/Y(II) (Supporting Information S1: Figure SM4C) showed lower values than in Col-0 (Supporting Information S1: Figure SM3B,C) in all oscillation amplitudes. Notably, the Y(I)/Y(II) of *pgrl1ab* showed a bumpy pattern in HL oscillation, with distinct decreases at about 70° and 280° phases, but a peak at approximately 180° phase (Supporting Information S1: Figure SM4C).

4 | DISCUSSION

4.1 | Regulation of qE occurs at all tested intensity ranges of oscillating light

Both the VDE- and PsbS-dependent qE components are indispensable in dealing with fluctuating light (Külheim & Jansson, 2005; Külheim et al., 2002; Sylak-Glassman et al., 2014). The rate of qE induction is governed by the PsbS-protein, but the amount of energy that can be quenched is determined by both PsbS- and VDE-dependent processes (Niu et al., 2023; Sylak-Glassman et al., 2014).

Our results here in 60 s period of oscillation support these previous findings: the Y(NPQ) of the *npq1* and *npq4* mutants was consistently lower than that of Col-0 across all amplitudes of oscillating light (Figure 2e). Thus, both VDE- and PsbS-dependent processes contribute to the qE in all intensities of light oscillations studied here.

Both *npq* mutants showed increased CET (Supporting Information S1: Figure SM3B,C), which aligns with less reduction of Fd in these mutants than in Col-0 (Figure 3b). This finding suggests that increased CET in the *npq* mutants (Supporting Information S1: -Figure SM3B,C) may represent a compensatory defence mechanism to counteract their inability to quench effectively. However, this increased CET in the *npq* mutants does not lead to increased photosynthesis control. If such control was present, it would be reflected in elevated Y(ND) (Figure 2b) and increased PC oxidation (Figure 3a) in the *npq* mutants compared to Col-0. Therefore, the apparent increase in CET, evaluated as Y(I)–Y(II) and Y(I)/Y(II), might be unreal and alternative electron transport (AET) routes (e.g. Mehler reaction) might contribute to the evaluated CET. Contribution of AET to the evaluated CET is expected owing to (i) the existing lateral heterogeneity of PSII and PSI (e.g. Tikhonov, 2023) and the fact that (ii) turnover time of PSII is about one order of magnitude slower (milliseconds; Ananayev & Dismukes, 2005; Crofts & Wraight, 1983) than that of PSI (a hundred of microseconds; Bottin & Mathis, 1985; Sétif & Bottin, 1995). With respect to (i), electrons from PSIs located in stroma lamellae can flow to AET and thus increase Y(I) but not affecting Y(II). With respect to (ii), faster turnover time of PSI, even if PSIs are located in the same TM of a granum as PSIIs, enables electron flow from PSIs to AET without affecting Y(II).

4.2 | The quantum yield of constitutive nonphotochemical quenching is not constant and depends on intensity of actinic light

The changes in the amplitude of Y(NPQ) in the *npq* mutants (Figure 2e) were accompanied by compensative quantitative changes of Y(NO) for all amplitudes of light oscillations (Figure 2f). Similar changes were also observed for Y(NO) and Y(NPQ) in the *pgrl1ab* mutant (Figure 4e,f). Moreover, the course of Y(NO) of both wild types in ML and HL oscillations, as well as that of the *pgrl1ab* and *crr2-2* mutants in HL oscillations (Figures 2f and 4f), deviated from the course of light oscillation and compensated to some extent for the delayed response of Y(NPQ) (Figures 2e and 4e). It means that the quantum yield of constitutive nonphotochemical quenching of excitation energy, Y(NO), which includes deactivation of the excitation energy via ChlF and via constitutive heat dissipation, is not constant at different light intensities and nonlinearly depends on light intensities. The fact that Y(NO) is not constant and appears to be 'regulated' has been noticed before (Han et al., 2022; Lazár et al., 2022). The simplest explanation for observed changes of Y(NO) might be attributed to the light-induced changes in Y(II) and Y(NPQ) since Y(NO) = 1 − Y(II) − Y(NPQ). However, it has been reported that changes in Y(NO) qualitatively agree with changes in ChlF signal during light oscillations and that TM voltage-dependent nonradiative charge recombination is probably involved in modulating the ChlF signal, and consequently Y(NO) (Lazár et al., 2022). Thus, the quantum yield of constitutive nonphotochemical quenching, Y(NO), also denoted as Y(f,D) (reviewed in Lazár, 2015) seems to be also regulated.

4.3 | The PGR5/PGRL1-CET is crucial in oscillating light of different amplitudes

Light changes with large magnitude were typically employed to investigate the role of CETs in response to light fluctuations (Kono & Terashima, 2016; Yamamoto & Shikanai, 2019; Yamori et al., 2016; Zhou et al., 2022), most of which can even lead to partial photoinhibition in wild-type organisms. In this study, we examined the physiological roles of PGR5/PGRL1-CET and NDH-like-CET in regulating photosynthesis under different amplitudes of light oscillations while applying the SPs during the oscillations. This way, we were able to explore the effects of these two CET pathways in detail during both the rising and declining phases of light intensity changes.

Regardless of the amplitudes of the light oscillations, *pgrl1ab* mutant showed a striking contrast to Col-0. It displayed higher Y(NA), lower Y(I) and Y(II), while Y(ND) remained at zero (Figure 4). This supports earlier findings that the absence of PGR5/PGRL1-CET causes severe PSI acceptor side limitation leading to a substantial reduction in the efficiency of both PSI and PSII under fluctuating light conditions (Shimakawa & Miyake, 2018; Suorsa et al., 2012, 2013; Yamamoto & Shikanai, 2019; Yamori et al., 2016). The marked reduction of Fd (Figure 5b) and PC (Figure 5a) further supports the notion that the entire electron transport chain is substantially reduced in the absence of PGR5/PGRL1-CET.

Interestingly, *pgrl1ab* mutant shows lower values of Y(I), Y(II) (Figure 4a,d) and a more reduced Fd (Figure 5b), and higher values of Y(NA) and Y(NPQ) (Figure 4c,e) at the end than in the beginning of the HL, but also ML oscillations. If qE is responsible for the higher values of Y(NPQ) (Figure 4e) at the end than in the beginning of the oscillations, a decreased proton efflux via ATP-synthase (Avenson et al., 2005; Degen et al., 2023) when PGR5/PGRL1-CET is malfunctioned, could be the reason for the accumulation of protons in lumen. However, it is more likely that the lower values of Y(I), Y(II) (Figure 4a,d) and the higher values of Y(NPQ) (Figure 4e) at the end than in the beginning of the oscillations reflect photoinhibition of PSI and PSII, and photoinhibitory nonphotochemical quenching, rather than qE. The lack of qE in the *pgrl1ab* mutant is also supported by the greater contribution of PGR5/PGRL1-CET to lumen acidification compared to NDH-like-CET (Degen et al., 2023; Kawashima et al., 2017; Wang et al., 2015). Thus, in agreement with the literature (Kono & Terashima, 2016; Kono et al., 2014; Shimakawa & Miyake, 2018; Yamamoto & Shikanai, 2019; Yamori et al., 2016; Zhou et al., 2022), our data indicates that PGR5/PGRL1-CET protects plants from photodamage in light fluctuations.

The decreased PC oxidation (Figure 5a), absence of Y(ND) (Figure 4b) and the decoupling of P700 redox state from PSII reduction found in *pgrl1ab* (Supporting Information S1: -Figure SM5A–C) collectively indicate that photosynthesis control at Cyt b6/f does not operate effectively in the absence of PGR5/PGRL1-CET, leading to electron congestion in PSI (Suorsa et al., 2012; Yamori & Shikanai, 2016). In wild-type plants, PGR5/PGRL1-CET plays a role in generating a pH difference across the TM (Kawashima et al., 2017; Wang et al., 2015), which is critical for supplying ATP required for downstream carbon fixation and for preventing photodamage (Ma, et al., 2021a). This is accomplished in wild types by inducing excess energy dissipation, as reflected in Y(NPQ) (Figure 4e) (Johnson et al., 2014; Müller et al., 2001), and by regulating the rate of electron transport via photosynthesis control (Supporting Information S1: Figure SM5A–C) (Suorsa et al., 2012; Yamori & Shikanai, 2016). However, neither of these mechanisms is functioning well in *pgrl1ab*. This suggests that lumen acidification in *pgrl1ab* was reduced (Degen et al., 2023; Kawashima et al., 2017; Wang et al., 2015), resulting in impaired photosynthesis control (Supporting Information S1: Figure SM5A–C) and restricted qE (Figure 4e).

4.4 | The NDH-like-CET acts as a safety valve to protect PSI in high amplitude of oscillating light

Despite significant advances in resolving its structure (Kouřil et al., 2014; Ma, et al., 2021b; Peltier et al., 2016), our understanding of the physiological role of NDH-like complex remains incomplete. The absence of NDH-like-CET led to a diversity of behaviours under different environmental stresses in different species (Yamori & Shikanai, 2016). Previous studies in *A. thaliana* showed mixed results regarding the impact of NDH-like-CET deficiency on photosynthetic performance under fluctuating light conditions. Some studies reported no significant difference compared to the wild types (Kono et al., 2014; Suorsa et al., 2012), while others found that the lack of NDH-like-CET limited PSI oxidation (Kono & Terashima, 2016; Shimakawa & Miyake, 2018; Zhou et al., 2022). The concept of NDH-like-CET as a safety valve was proposed previously based on the observation that double mutants defective in both PGR5/PGRL1-CET and NDH-like-CET exhibited greater suppression of pmf accumulation, P700 oxidation and lower electron transport efficiency in constant light than single mutants lacking PGR5/PGRL1-CET (Munekage et al., 2004; Nakano et al., 2019; Wang et al., 2015; Yamamoto et al., 2011). However, taken together with the fact that single mutant defective in NDH-like CET showed in these studies only small differences when compared with the wild types, the lack of NDH-like CET can be probably (partly) compensated by PGR5/PGRL1 CET. Here, we directly demonstrated the safety valve function of NDH-like-CET by comparing the performance of multiple components in the electron transport chain between the *crr2-2* mutant and its wild-type Col-*gl1*, under different amplitudes of light oscillations.

In the present study, *crr2-2* exhibited limitations on the PSI acceptor side, particularly pronounced during the light rising phase of HL oscillation (Figures 4c and 5b), whereas the PSI donor side was less limiting than in Col-*gl1* (Figures 4b and 5a). These differences were observed under oscillating light of all three amplitudes (LL, ML and HL), but not during the light response curve measurements (Figure 1b,c,h,i). In the case of HL oscillation, we noted that the initial increase in Y(NA), accompanied by a shallow depression phase of Y (ND) (Figure 4b), was partly alleviated as the intensity of oscillating light approached its maximum at a 180° phase (Figure 4c). Such dynamic redox changes in the PSI donor and acceptor sides are difficult to monitor in a rectangular light condition, where light intensity changes abruptly (Kono & Terashima, 2016; Zhou et al., 2022). The decline of Y(NA) at the phase of maximal light intensity in HL oscillation may reflect enhancement of PGR5/PGRL1-CET (Supporting Information S1: Figure SM4B,C) or AETs (see the reasoning above), such as the Mehler reaction, which could compensate for the NDH-like-CET defect.

Interestingly, the *crr2-2* mutant showed consistently higher Y(NPQ) and NPQ parameter than Col-*gl1* at all oscillating light conditions (Figure 4e and SM4A). This was also observed by Shimakawa and Miyake (2018) under oscillating light with the same period but higher amplitude (30–1970 µmol photons m^{-2} s^{-1}), whereas it was not the case under rectangular light changes, where Y(NPQ) in *crr2-2* was roughly the same as in its wild type (Kono & Terashima, 2016; Zhou et al., 2022). The NDH-like complex is able to transport electrons from Fd to plastoquinone while simultaneously causing accumulation of protons in lumen, not only via oxidation of reduced plastoquinone molecules at Cyt b6/f but also by transporting protons from stroma to lumen by itself (Kouřil et al., 2014; Laughlin et al., 2020; Strand et al., 2017). Despite this expected superior proton transport ability of the NDH-like complex, its absence does not apparently impair the induction of qE, suggesting a low turnover rate of the NDH-like-CET (Joliot & Joliot, 2005; Okegawa et al., 2008). Linear electron transport and the PGR5/PGRL1-CET, along with other AETs, may already be sufficient to decrease luminal pH and induce qE, especially for light intensities exceeding 200 µmol photons m^{-2} s^{-1} (Nakano et al., 2019).

To further elucidate the impact of the absence of NDH-like-CET on luminal pH, we also assessed the correlation between qP and P700 reduction (Supporting Information S1: Figure SM5A–C), which mirrors the state of photosynthesis control. Under HL oscillation, *crr2-2* had more reduced PSI compared to Col-*gl1* while maintaining the same PSII openness (Supporting Information S1: Figure SM5A); this effect was, however, not visible in ML and LL oscillations (Supporting Information S1: Figure SM5B,C). It seems that the absence of NDH-like-CET may moderately retard lumen acidification, and consequently, the induction of photosynthesis control under HL oscillation. However, this absence does not appear to affect the induction of qE (Figure 4e). This agrees with the facts that pmf is only slightly lower in mutants lacking NDH-like-CET compared to wild type (Wang et al., 2015) and that NDH-like-CET contributes only by about 5% to the total ΔpH across the TM (Kawashima et al., 2017). It is also consistent with the fact that qE requires less acidified lumen than the photosynthesis control does (Schansker, 2022).

These findings collectively suggest that the NDH-like-CET may function as a safety valve when the amplitude of light oscillations is

high, alleviating the electron pressure on the PSI acceptor side and enhancing ΔpH formation across TM, thereby effectively inducing photosynthesis control. Furthermore, under conditions where photosynthesis control was less obvious such as in LL and ML oscillations (Supporting Information S1: Figure SM5B,C), the absence of NDH-like-CET in *crr2-2* resulted in more reduced PSI donor and acceptor sides (Figure 5) and slightly lower Y(I) and Y(II) (Figure 4a,d). This suggests that NDH-like-CET may contribute to the maintenance of efficient linear electron transport under these conditions. While not indispensable, the NDH-like-CET does support rapid regulations in response to oscillating light, which is essential for optimising photosynthesis in dynamically changing light environments.

4.5 | Complementary effects among multiple protective regulatory mechanisms

Long-term acclimation to fluctuating light involves alterations in gene expression and protein abundance (Alter et al., 2012; Barker et al., 1997; Gjindali et al., 2021; Schneider et al., 2019; Vialet-Chabrand et al., 2017; Wei et al., 2021), resulting in enhanced regulatory mechanisms. Plants grown in fluctuating light have increased qE, attributed to higher amounts of PsbS protein and enzymes involved in the xanthophyll cycle, compared to plants grown under constant light (Alter et al., 2012; Caliandro et al., 2013; Schneider et al., 2019; Wei et al., 2021). Some genes and proteins associated with NDH-like-CET and PGR5/PGRL1-CET are also upregulated in response to long-term fluctuating light (Niedermaier et al., 2020; Schneider et al., 2019; Suorsa et al., 2012).

In this study, plants grown under constant low light were exposed to oscillating light only during measurements. This short-term light oscillation revealed rapid complementary effects among different protective mechanisms, particularly pronounced in mutants lacking one or the other regulatory mechanisms. Further studies are required to explore these interactions. Here is a brief summary of observed interplays among multiple regulatory processes in tested oscillating light conditions:

- The complementary effect between Y(NPQ) and Y(NO) as discussed above can be observed in all tested genotypes (Figures 2e,f and 4e,f).
- Although the decrease of Y(NPQ) in the qE-deficient mutants was largely counteracted by increased Y(NO) under oscillating light (Figure 2e,f), there was still a slight reduction in PSII efficiency in these mutants (Figure 2d). However, these defects had little impact on PSI efficiency (Figure 2a), even in HL oscillation. This may be attributed to an increased efficiency of CET in *npq* mutants, evident via higher Y(I)–Y(II) and Y(I)/Y(II) levels (Supporting Information S1: Figure SM3B,C), as well as less reduced Fd (Figure 3b) compared to their wild type. The contribution of AETs can also be considered.
- In HL oscillations, the PSI acceptor side limitation of *crr2-2* was temporarily induced during the light ascending phase (Figures 4c and 5b). We speculate that PGR5/PGRL1-CET or other AETs, for example, the malate valve or the Mehler reaction (Lazár et al., 2022), might alleviate this limitation on the acceptor side of PSI, causing it to diminish within seconds of its induction (Figure 4c).
- The *crr2-2* mutant had higher levels of Y(NPQ) and NPQ parameter than Col-*gl1* at all tested oscillation amplitudes (Figure 4e and SM4A), likely serving to prevent over-excitation of photosystems.
- The peak of Y(I)/Y(II) in *pgrl1ab* between 90° and 270° phases of HL oscillation (Supporting Information S1: Figure SM4C) may be partially attributed to the effective functioning of NDH-like-CET or other AETs under equivalent conditions.

In this study, we delved into the dynamics of two short-term regulatory mechanisms, qE and CET, in response to different amplitudes of oscillating light. Their interplays are already dazzling. However, they constitute only a small part of the intricate regulatory networks adjusting and optimising photosynthesis, which operate across a wide range of scales. Photosynthesis and its regulatory networks are highly complex and integrated. To gain a deeper understanding of this complexity in natural environments necessitates the study of the dynamic response of photosynthesis and its regulation to fluctuating light or, more broadly, to a dynamically changing environment (Cruz et al., 2016; Gjindali et al., 2021). Many experimental investigations have been conducted under well-defined light conditions, drastically differing from natural light environments. Therefore, it is crucial to explore novel approaches for systematically investigating the dynamics of photosynthesis in changing light environments. Our findings highlight the potential of harmonically oscillating light approach in advancing the study of the dynamics of photosynthesis.

ACKNOWLEDGEMENTS

The authors thank Dr. Benjamin Bailleul for his comments. The authors thank Toshiharu Shikanai of Kyoto University, Japan for kindly providing seeds of the *crr2-2* mutant of *Arabidopsis thaliana* and Dario Leister in Ludwig Maximilian University München, Germany for providing seeds of the *pgrl1ab* mutant. D. L. and L. N. were supported by the European Regional Development Fund project 'Plants as a tool for sustainable global development' (no. CZ.02.1.01/0.0/0.0/16_019/0000827) and the Horizon Europe, European Innovation Council Pathfinder Open 2021 project 'DREAM' (no. 101046451). S. M. was also supported by the Horizon Europe, European Innovation Council Pathfinder Open 2021 project 'DREAM' (no. 101046451). Y. N. gratefully acknowledges the financial support from the Federal Ministry of Education and Research of Germany (BMBF) in the 'YESPVNIGBEN' project (no. 03SF0576A). Open access publishing facilitated by Univerzita Palackeho v Olomouci, as part of the Wiley - CzechELib agreement.

CONFLICT OF INTEREST STATEMENT

The authors declare no conflict of interest.

ORCID

Yuxi Niu http://orcid.org/0000-0002-9627-9864
Shizue Matsubara http://orcid.org/0000-0002-1440-6496
Ladislav Nedbal http://orcid.org/0000-0002-4282-3406
Dušan Lazár http://orcid.org/0000-0001-8035-4017

REFERENCES

Allahverdiyeva, Y., Suorsa, M., Tikkanen, M. & Aro, E.-M. (2015) Photoprotection of photosystems in fluctuating light intensities. *Journal of Experimental Botany*, 66(9), 2427–2436. Available from: https://doi.org/10.1093/jxb/eru463

Alter, P., Dreissen, A., Luo, F.L. & Matsubara, S. (2012) Acclimatory responses of Arabidopsis to fluctuating light environment: comparison of different sunfleck regimes and accessions. *Photosynthesis Research*, 113(1–3), 221–237. Available from: https://doi.org/10.1007/s11120-012-9757-2

Ananyev, G. & Dismukes, G.C. (2005) How fast can photosystem II split water? Kinetic performance at high and low frequencies. *Photosynthesis Research*, 84(1–3), 355–365. Available from: https://doi.org/10.1007/s11120-004-7081-1

Avenson, T.J., Cruz, J.A., Kanazawa, A. & Kramer, D.M. (2005) Regulating the proton budget of higher plant photosynthesis. *Proceedings of the National Academy of Sciences USA*, 102(27), 9709–9713. Available from https://doi.org/10.1073/pnas.0503952102

Barker, D.H., Logan, B.A., III, W.W.A. & Demmig-Adams, B. (1997) The response of xanthophyll cycle-dependent energy dissipation in *Alocasia brisbanensis* to sunflecks in a subtropical rainforest *Funct. Plant Biology*, 24(1), 27–33. Available from: https://doi.org/10.1071/PP96059

Bottin, H. & Mathis, P. (1985) Interaction of plastocyanin with the photosystem I reaction center: a kinetic study by flash absorption spectroscopy. *Biochemistry*, 24(23), 6453–6460. Available from: https://doi.org/10.1021/bi00344a022

Chazdon, R.L. & Pearcy, R.W. (1991) The importance of sunflecks for forest understory plants. *Bioscience*, 41(11), 760–766. Available from: https://doi.org/10.2307/1311725

Caliandro, R., Nagel, K.A., Kastenholz, B., Bassi, R., Li, Z., Niyogi, K.K. et al. (2013) Effects of altered α- and β-branch carotenoid biosynthesis on photoprotection and whole-plant acclimation of Arabidopsis to photo-oxidative stress. *Plant, Cell & Environment*, 36(2), 438–453. Available from: https://doi.org/10.1111/j.1365-3040.2012.02586.x

Crofts, A.R.andWraight, C.A. (1983) The electrochemical domain of photosynthesis. *Biochimica et Biophysica Acta (BBA)—Reviews on Bioenergetics*, 726(3), 149–185. Available from: https://doi.org/10.1016/0304-4173(83)90004-6

Cruz, J.A., Savage, L.J., Zegarac, R., Hall, C.C., Satoh-Cruz, M., Davis, G.A. et al. (2016) Dynamic environmental photosynthetic imaging reveals emergent phenotypes. *Cell Systems*, 2(6), 365–377. Available from: https://doi.org/10.1016/j.cels.2016.06.001

DalCorso, G., Pesaresi, P., Masiero, S., Aseeva, E., Schünemann, D., Finazzi, G. et al. (2008) A complex containing PGRL1 and PGR5 is involved in the switch between linear and cyclic electron flow in Arabidopsis. *Cell*, 132(2), 273–285. Available from: https://doi.org/10.1016/j.cell.2007.12.028

Degen, G.E., Jackson, P.J., Proctor, M.S., Zoulias, N., Casson, S.A. & Johnson, M.P. (2023) High cyclic electron transfer via the PGR5 pathway in the absence of photosynthetic control. *Plant Physiology*, 192(1), 370–386. Available from: https://doi.org/10.1093/plphys/kiad084

Demmig-Adams, B. (1990) Carotenoids and photoprotection in plants: a role for the xanthophyll zeaxanthin. *Biochimica et Biophysica Acta (BBA)—Bioenergetics*, 1020(1), 1–24. Available from: https://doi.org/10.1016/0005-2728(90)90088-L

Demmig-Adams, B., Garab, G., Adams, W. & Govindjee, U. (2014) *Non-photochemical quenching and energy dissipation in plants, algae and cyanobacteria preface*. Netherlands: Springer.

Durand, M. & Robson, T.M. (2023) Fields of a thousand shimmers: canopy architecture determines high-frequency light fluctuations. *New Phytologist*, 238(5), 2000–2015. Available from: https://doi.org/10.1111/nph.18822

Duysens, L.N.M. & Sweers, H.E. (1963) Mechanism of the two photochemical reactions in algaeas studied by means of fluorescence In: Japanese society of plant physiologists (Ed.). *Studies on microalgae and photosynthetic bacteria* Tokyo: University of Tokyo Press. pp. 353–372.

Ferimazova, N., Küpper, H., Nedbal, L. & Trtílek, M. (2002) New insights into photosynthetic oscillations revealed by two-dimensional microscopic measurements of chlorophyll fluorescence kinetics in intact leaves and isolated protoplasts. *Photochemistry and Photobiology*, 76(5), 501–508. Available from: https://doi.org/10.1562/0031-8655(2002)0760501NIIPOR2.0.CO2

Garab, G., Magyar, M., Sipka, G. & Lambrev, P.H. (2023) New foundations for the physical mechanism of variable chlorophyll a fluorescence. Quantum efficiency versus the light-adapted state of photosystem II. *Journal of Experimental Botany*, 74(18), 5458–5471. Available from: https://doi.org/10.1093/jxb/erad252

Gilmore, A.M. (1997) Mechanistic aspects of xanthophyll cycle-dependent photoprotection in higher plant chloroplasts and leaves. *Physiologia Plantarum*, 99(1), 197–209. Available from: https://doi.org/10.1034/j.1399-3054.1997.990127.x

Gjindali, A., Herrmann, H.A., Schwartz, J.-M., Johnson, G.N. & Calzadilla, P.I. (2021) A holistic approach to study photosynthetic acclimation responses of plants to fluctuating light. *Frontiers in Plant Science*, 12, 668512. Available from: https://doi.org/10.3389/fpls.2021.668512

Han, J., Chang, C.Y.Y., Gu, L., Zhang, Y., Meeker, E.W., Magney, T.S. et al. (2022) The physiological basis for estimating photosynthesis from Chla fluorescence. *New Phytologist*, 234(4), 1206–1219. Available from: https://doi.org/10.1111/nph.18045

Hashimoto, M., Endo, T., Peltier, G., Tasaka, M. & Shikanai, T. (2003) A nucleus-encoded factor, CRR2, is essential for the expression of chloroplast ndhB in Arabidopsis. *The Plant Journal*, 36(4), 541–549. Available from: https://doi.org/10.1046/j.1365-313X.2003.01900.x

Hertle, A.P., Blunder, T., Wunder, T., Pesaresi, P., Pribil, M., Armbruster, U. et al. (2013) PGRL1 is the elusive ferredoxin-plastoquinone reductase in photosynthetic cyclic electron flow. *Molecular Cell*, 49(3), 511–523. Available from: https://doi.org/10.1016/J.MOLCEL.2012.11.030

Holzwarth, A.R., Miloslavina, Y., Nilkens, M. & Jahns, P. (2009) Identification of two quenching sites active in the regulation of photosynthetic light-harvesting studied by time-resolved fluorescence. *Chemical Physics Letters*, 483(4–6), 262–267. Available from: https://doi.org/10.1016/j.cplett.2009.10.085

Huang, W., Zhang, S.-B. & Cao, K.-F. (2011) Cyclic electron flow plays an important role in photoprotection of tropical trees illuminated at temporal chilling temperature. *Plant and Cell Physiology*, 52(2), 297–305. Available from: https://doi.org/10.1093/pcp/pcq166

Ikeuchi, M., Uebayashi, N., Sato, F. & Endo, T. (2014) Physiological functions of PsbS-dependent and PsbS-independent NPQ under naturally fluctuating light conditions. *Plant and Cell Physiology*, 55(7), 1286–1295. Available from: https://doi.org/10.1093/pcp/pcu069

Jahns, P. & Holzwarth, A.R. (2012) The role of the xanthophyll cycle and of lutein in photoprotection of photosystem II. *Biochimica et Biophysica Acta (BBA)—Bioenergetics*, 1817(1), 182–193. Available from: https://doi.org/10.1016/j.bbabio.2011.04.012

Johnson, G.N. (2011) Physiology of PSI cyclic electron transport in higher plants. *Biochimica et Biophysica Acta (BBA)—Bioenergetics*, 1807(3), 384–389. Available from: https://doi.org/10.1016/j.bbabio.2010.11.009

Johnson, G.N., Cardol, P., Minagawa, J. & Finazzi, G. (2014) Regulation of electron transport in photosynthesis. In: Theg, S.M. & Wollman, F.-A. (Eds.) *Plastid biology*. New York: Springer, pp. 437–464. Available from: https://doi.org/10.1007/978-1-4939-1136-3_16

Joliot, P. & Joliot, A. (2005) Quantification of cyclic and linear flows in plants. *Proceedings of the National Academy of Sciences of the United States of America*, 102(13), 4913–4918. Available from: https://doi.org/10.1073/pnas.0501268102

Kaiser, E., Morales, A. & Harbinson, J. (2018) Fluctuating light takes crop photosynthesis on a rollercoaster ride. *Plant Physiology*, 176(2), 977–989. Available from: https://doi.org/10.1104/pp.17.01250

Kawashima, R., Sato, R., Harada, K. & Masuda, S. (2017) Relative contributions of PGR5- and NDH-dependent photosystem I cyclic electron flow in the generation of a proton gradient in Arabidopsis chloroplasts. *Planta*, 246(5), 1045–1050. Available from: https://doi.org/10.1007/s00425-017-2761-1

Klughammer, C. & Schreiber, U. (2016) Deconvolution of ferredoxin, plastocyanin, and P700 transmittance changes in intact leaves with a new type of kinetic LED array spectrophotometer. *Photosynthesis Research*, 128(2), 195–214. Available from: https://doi.org/10.1007/s11120-016-0219-0

Kono, M., Noguchi, K. & Terashima, I. (2014) Roles of the cyclic electron flow around PSI (CEF-PSI) and O_2-dependent alternative pathways in regulation of the photosynthetic electron flow in short-term fluctuating light in Arabidopsis thaliana. *Plant and Cell Physiology*, 55(5), 990–1004. Available from: https://doi.org/10.1093/pcp/pcu033

Kono, M. & Terashima, I. (2014) Long-term and short-term responses of the photosynthetic electron transport to fluctuating light. *Journal of Photochemistry and Photobiology, B: Biology*, 137, 89–99. Available from: https://doi.org/10.1016/j.jphotobiol.2014.02.016

Kono, M. & Terashima, I. (2016) Elucidation of photoprotective mechanisms of PSI against fluctuating light photoinhibition. *Plant & Cell Physiology*, 57(7), 1405–1414. Available from: https://doi.org/10.1093/pcp/pcw103

Kouřil, R., Strouhal, O., Nosek, L., Lenobel, R., Chamrád, I., Boekema, E.J. et al. (2014) Structural characterization of a plant photosystem I and NAD(P)H dehydrogenase supercomplex. *The Plant Journal*, 77(4), 568–576. Available from: https://doi.org/10.1111/tpj.12402

Kromdijk, J., Głowacka, K., Leonelli, L., Gabilly, S.T., Iwai, M., Niyogi, K.K. et al. (2016) Improving photosynthesis and crop productivity by accelerating recovery from photoprotection. *Science*, 354(6314), 857–861. Available from: https://doi.org/10.1126/science.aai8878

Külheim, C., Ågren, J. & Jansson, S. (2002) Rapid regulation of light harvesting and plant fitness in the field. *Science*, 297(5578), 91–93. Available from: https://doi.org/10.1126/science.1072359

Külheim, C. & Jansson, S. (2005) What leads to reduced fitness in non-photochemical quenching mutants? *Physiologia Plantarum*, 125(2), 202–211. Available from: https://doi.org/10.1111/j.1399-3054.2005.00547.x

Laisk, A. & Oja, V. (2020) Variable fluorescence of closed photochemical reaction centers. *Photosynthesis Research*, 143(3), 335–346. Available from: https://doi.org/10.1007/s11120-020-00712-3

Laughlin, T.G., Savage, D.F. & Davies, K.M. (2020) Recent advances on the structure and function of NDH-1: the complex I of oxygenic photosynthesis. *Biochimica et Biophysica Acta (BBA)—Bioenergetics*, 1861(11), 148254. Available from:https://doi.org/10.1016/J.BBABIO.2020.148254

Lazár, D. (2015) Parameters of photosynthetic energy partitioning. *Journal of Plant Physiology*, 175, 131–147. Available from: https://doi.org/10.1016/j.jplph.2014.10.021

Lazár, D., Kaňa, R., Klinkovský, T. & Nauš, J. (2005) Experimental and theoretical study on high temperature induced changes in chlorophyll a fluorescence oscillations in barley leaves upon 2 % CO_2. *Photosynthetica*, 43(1), 13–27. Available from: https://doi.org/10.1007/s11099-005-3027-x

Lazár, D., Niu, Y. & Nedbal, L. (2022) Insights on the regulation of photosynthesis in pea leaves exposed to oscillating light. *Journal of Experimental Botany*, 73(18), 6380–6393. Available from: https://doi.org/10.1093/jxb/erac283

Li, X.P., Björkman, O., Shih, C., Grossman, A.R., Rosenquist, M., Jansson, S. et al. (2000) A pigment-binding protein essential for regulation of photosynthetic light harvesting. *Nature*, 403(6768), 391–395. Available from: https://doi.org/10.1038/35000131

Li, X.-P., Müller-Moulé, P., Gilmore, A.M. & Niyogi, K.K. (2002) PsbS-dependent enhancement of feedback de-excitation protects photosystem II from photoinhibition. *Proceedings of the National Academy of Sciences of the United States of America*, 99(23), 15222–15227. Available from: https://doi.org/10.1073/pnas.232447699

Ma, M., Liu, Y., Bai, C., Yang, Y., Sun, Z., Liu, X. et al. (2021) The physiological functionality of PGR5/PGRL1-dependent cyclic electron transport in sustaining photosynthesis. *Frontiers of Plant Science*, 12, 702196. Available from: https://doi.org/10.3389/fpls.2021.702196

Ma, M., Liu, Y., Bai, C. & Yong, J.W.H. (2021) The significance of chloroplast NAD(P)H dehydrogenase complex and its dependent cyclic electron transport in photosynthesis. *Frontiers of Plant Science*, 12, 661863.

Magyar, M., Sipka, G., Kovács, L., Ughy, B., Zhu, Q., Han, G. et al. (2018) Rate-limiting steps in the dark-to-light transition of photosystem II—revealed by chlorophyll-*a* fluorescence induction. *Scientific Reports*, 8(1), 2755. Available from: https://doi.org/10.1038/s41598-018-21195-2

Miyake, C., Miyata, M., Shinzaki, Y. & Tomizawa, K. (2005) CO2 response of cyclic electron flow around PSI (CEF-PSI) in tobacco leaves—relative electron fluxes through PSI and PSII determine the magnitude of non-photochemical quenching (NPQ) of chl fluorescence. *Plant and Cell Physiology*, 46(4), 629–637. Available from: https://doi.org/10.1093/pcp/pci067

Morales, A. & Kaiser, E. (2020) Photosynthetic acclimation to fluctuating irradiance in plants. *Frontiers in Plant Science*, 11, 268. Available from: https://doi.org/10.3389/FPLS.2020.00268/BIBTEX

Müller, P., Li, X.-P. & Niyogi, K.K. (2001) Non-photochemical quenching. A response to excess light energy. *Plant Physiology*, 125(4), 1558–1566. Available from: https://doi.org/10.1104/pp.125.4.1558

Munekage, Y., Hashimoto, M., Miyake, C., Tomizawa, K.I., Endo, T., Tasaka, M. et al. (2004) Cyclic electron flow around photosystem I is essential for photosynthesis. *Nature*, 429(6991), 579–582. Available from: https://doi.org/10.1038/nature02598

Munekage, Y., Hojo, M., Meurer, J., Endo, T., Tasaka, M. & Shikanai, T. (2002) PGR5 is involved in cyclic electron flow around photosystem I and is essential for photoprotection in Arabidopsis. *Cell*, 110(3), 361–371. Available from: https://doi.org/10.1016/S0092-8674(02)00867-X

Nakano, H., Yamamoto, H. & Shikanai, T. (2019) Contribution of NDH-dependent cyclic electron transport around photosystem I to the generation of proton motive force in the weak mutant allele of pgr5. *Biochimica et Biophysica Acta (BBA)—Bioenergetics*, 1860(5), 369–374. Available from: https://doi.org/10.1016/j.bbabio.2019.03.003

Nedbal, L. & Březina, V. (2002) Complex metabolic oscillations in plants forced by harmonic irradiance. *Biophysical Journal*, 83(4), 2180–2189. Available from: https://doi.org/10.1016/S0006-3495(02)73978-7

Nedbal, L., Březina, ě, Adamec, F., Štys, D., Oja, V., Laisk, A. et al. (2003) Negative feedback regulation is responsible for the non-linear modulation of photosynthetic activity in plants and cyanobacteria exposed to a dynamic light environment. *Biochimica et Biophysica Acta (BBA)—Bioenergetics*, 1607(1), 5–17. Available from: https://doi.org/10.1016/j.bbabio.2003.08.005

Nedbal, L., Březina, V., Červený, J. & Trtílek, M. (2005) Photosynthesis in dynamic light: systems biology of unconventional chlorophyll fluorescence transients in Synechocystis sp. PCC 6803. *Photosynthesis Research*, 84(1–3), 99–106. Available from: https://doi.org/10.1007/s11120-004-6428-y

Nedbal, L. & Lazár, D. (2021) Photosynthesis dynamics and regulation sensed in the frequency domain. *Plant Physiology*, 187(2), 646–661. Available from: https://doi.org/10.1093/plphys/kiab317

Niedermaier, S., Schneider, T., Bahl, M.O., Matsubara, S. & Huesgen, P.F. (2020) Photoprotective acclimation of the Arabidopsis thaliana leaf proteome to fluctuating light. *Frontiers in Genetics*, 11, 154. Available from: https://doi.org/10.3389/fgene.2020.00154

Niu, Y., Lazár, D., Holzwarth, A.R., Kramer, D.M., Matsubara, S., Fiorani, F. et al. (2023) Plants cope with fluctuating light by frequency-dependent non-photochemical quenching and cyclic electron transport. *New Phytologist*, 239(5), 1869–1886. Available from: https://doi.org/10.1111/nph.19083

Niyogi, K.K., Grossman, A.R. & Björkman, O. (1998) Arabidopsis mutants define a central role for the xanthophyll cycle in the regulation of photosynthetic energy conversion. *The Plant Cell*, 10(7), 1121–1134. Available from: https://doi.org/10.1105/tpc.10.7.1121

Oja, V. & Laisk, A. (2020) Time- and reduction-dependent rise of photosystem II fluorescence during microseconds-long inductions in leaves. *Photosynthesis Research*, 145(3), 209–225. Available from: https://doi.org/10.1007/s11120-020-00783-2

Okegawa, Y., Kagawa, Y., Kobayashi, Y. & Shikanai, T. (2008) Characterization of factors affecting the activity of photosystem I cyclic electron transport in chloroplasts. *Plant and Cell Physiology*, 49(5), 825–834. Available from: https://doi.org/10.1093/pcp/pcn055

Peltier, G., Aro, E.M. & Shikanai, T. (2016) NDH-1 and NDH-2 plastoquinone reductases in oxygenic photosynthesis. *Annual Review of Plant Biology*, 67, 55–80. Available from: https://doi.org/10.1146/annurev-arplant-043014-114752

Roach, T. & Krieger-Liszkay, A. (2012) The role of the PsbS protein in the protection of photosystems I and II against high light in Arabidopsis thaliana. *Biochimica et Biophysica Acta (BBA)—Bioenergetics*, 1817(12), 2158–2165. Available from: https://doi.org/10.1016/j.bbabio.2012.09.011

Roden, J.S. & Pearcy, R.W. (1993) Effect of leaf flutter on the light environment of poplars. *Oecologia*, 93(2), 201–207. Available from: https://doi.org/10.1007/bf00317672

Rumberg, B. & Siggel, U. (1969) pH changes in the inner phase of the thylakoids during photosynthesis. *Die Naturwissenschaften*, 56(3), 130–132. Available from: https://doi.org/10.1007/BF00601025

Ruban, A.V. (2016) Nonphotochemical chlorophyll fluorescence quenching: mechanism and effectiveness in protecting plants from photodamage. *Plant Physiology*, 170(4), 1903–1916. Available from: https://doi.org/10.1104/pp.15.01935

Sagun, J.V., Badger, M.R., Chow, W.S. & Ghannoum, O. (2019) Cyclic electron flow and light partitioning between the two photosystems in leaves of plants with different functional types. *Photosynthesis Research*, 142(3), 321–334. Available from: https://doi.org/10.1007/s11120-019-00666-1

Sazanov, L.A., Burrows, P.A. & Nixon, P.J. (1998) The chloroplast Ndh complex mediates the dark reduction of the plastoquinone pool in response to heat stress in tobacco leaves. *FEBS Letters*, 429(1), 115–118. Available from: https://doi.org/10.1016/S0014-5793(98)00573-0

Schansker, G. (2022) Determining photosynthetic control, a probe for the balance between electron transport and Calvin-Benson cycle activity, with the DUAL-KLAS-NIR. *Photosynthesis Research*, 153, 191–204. Available from: https://doi.org/10.1007/s11120-022-00934-7

Schansker, G., Tóth, S.Z., Kovács, L., Holzwarth, A.R. & Garab, G. (2011) Evidence for a fluorescence yield change driven by a light-induced conformational change within photosystem II during the fast chlorophyll a fluorescence rise. *Biochimica et Biophysica Acta (BBA) - Bioenegetics*, 1807(9), 1032–1043. Available from: https://doi.org/10.1016/j.bbabio.2011.05.022

Schneider, T., Bolger, A., Zeier, J., Preiskowski, S., Benes, V., Trenkamp, S. et al. (2019) Fluctuating light interacts with time of day and leaf development stage to reprogram gene expression. *Plant Physiology*, 179(4), 1632–1657. Available from: https://doi.org/10.1104/PP.18.01443

Schreiber, U. (2004) Pulse-amplitude-modulation (PAM) fluorometry and saturation pulse method: an overview. In: Papageorgiou, G.C. & Govindjee, G. (Eds.) *Chlorophyll a fluorescence: a signature of photosynthesis*. Dordrecht: Springer, pp. 279–319.

Schreiber, U. & Klughammer, C. (2016) Analysis of photosystem I donor and acceptor sides with a new type of online-deconvoluting kinetic LED-array spectrophotometer. *Plant & Cell Physiology*, 57(7), 1454–1467. Available from: https://doi.org/10.1093/pcp/pcw044

Setif, P.Q.Y. & Bottin, H. (1995) Laser flash absorption spectroscopy study of ferredoxin reduction by photosystem I: spectral and kinetic evidence for the existence of several photosystem I-ferredoxin complexes. *Biochemistry*, 34(28), 9059–9070. Available from: https://doi.org/10.1021/bi00028a015

Shikanai, T. (2014) Central role of cyclic electron transport around photosystem I in the regulation of photosynthesis. *Current Opinion in Biotechnology*, 26, 25–30. Available from: https://doi.org/10.1016/J.COPBIO.2013.08.012

Shikanai, T. & Okegawa, Y. (2008) Regulation of photosynthesis via PSI cyclic electron transport. In: Allen, J.F., Gantt, E., Golbeck, J.H. & Osmond, B. (Eds.) *Photosynthesis. Energy from the Sun*. Dordrecht: Springer, pp. 981–985.

Shimakawa, G. & Miyake, C. (2018) Changing frequency of fluctuating light reveals the molecular mechanism for P700 oxidation in plant leaves. *Plant Direct*, 2(7), e00073. Available from: https://doi.org/10.1002/pld3.73

Siggel, U. (1976) The function of plastoquinone as electron and proton carrier in photosynthesis. *Bioelectrochemistry and Bioenergetics*, 3(2), 302–318. Available from: https://doi.org/10.1016/0302-4598(76)80012-8

Sipka, G., Magyar, M., Mezzetti, A., Akhtar, P., Zhu, Q., Xiao, Y. et al. (2021) Light-adapted charge-separated state of photosystem II: structural and functional dynamics of the closed reaction center. *The Plant Cell*, 33(4), 1286–1302. Available from: https://doi.org/10.1093/plcell/koab008

Smith, W.K. & Berry, Z.C. (2013) Sunflecks? *Tree Physiology*, 33(3), 233–237. Available from: https://doi.org/10.1093/treephys/tpt005

Steen, C.J., Morris, J.M., Short, A.H., Niyogi, K.K. & Fleming, G.R. (2020) Complex roles of PsbS and xanthophylls in the regulation of nonphotochemical quenching in Arabidopsis thaliana under fluctuating light. *The Journal of Physical Chemistry B*, 124(46), 10311–10325. Available from: https://doi.org/10.1021/acs.jpcb.0c06265

Stirbet, A. (2013) Excitonic connectivity between photosystem II units: what is it, and how to measure it. *Photosynthesis Research*, 116(2–3), 189–214. Available from: https://doi.org/10.1007/s11120-013-9863-9

Strand, D.D., Fisher, N. & Kramer, D.M. (2017) The higher plant plastid NAD(P)H dehydrogenase-like complex (NDH) is a high efficiency proton pump that increases ATP production by cyclic electron flow. *Journal of Biological Chemistry*, 292(28), 11850–11860. Available from: https://doi.org/10.1074/jbc.M116.770792

Sugimoto, K., Okegawa, Y., Tohri, A., Long, T.A., Covert, S.F., Hisabori, T. et al. (2013) A single amino acid alteration in PGR5 confers resistance to antimycin A in cyclic electron transport around PSI. *Plant and Cell Physiology*, 54(9), 1525–1534. Available from: https://doi.org/10.1093/pcp/pct098

Suorsa, M., Grieco, M., Järvi, S., Gollan, P.J., Kangasjärvi, S., Tikkanen, M. et al. (2013) PGR5 ensures photosynthetic control to safeguard photosystem I under fluctuating light conditions. *Plant Signaling & Behavior*, 8(1), e22741. Available from: https://doi.org/10.4161/psb.22741

Suorsa, M., Järvi, S., Grieco, M., Nurmi, M., Pietrzykowska, M., Rantala, M. et al. (2012) PROTON GRADIENT REGULATION5 is essential for proper acclimation of Arabidopsis photosystem I to naturally and artificially fluctuating light conditions. *The Plant Cell*, 24(7), 2934–2948. Available from: https://doi.org/10.1105/tpc.112.097162

Sylak-Glassman, E.J., Malnoë, A., De Re, E., Brooks, M.D., Fischer, A.L., Niyogi, K.K. et al. (2014) Distinct roles of the photosystem II protein PsbS and zeaxanthin in the regulation of light harvesting in plants revealed by fluorescence lifetime snapshots. *Proceedings of the National Academy of Sciences of the United States of America*, 111(49), 17498–17503. Available from: https://doi.org/10.1073/pnas.1418317111

Takagi, D., Takumi, S., Hashiguchi, M., Sejima, T. & Miyake, C. (2016) Superoxide and singlet oxygen produced within the thylakoid membranes both cause photosystem I photoinhibition. *Plant Physiology*, 171(3), 1626–1634. Available from: https://doi.org/10.1104/pp.16.00246

Terashima, I., Funayama, S. & Sonoike, K. (1994) The site of photoinhibition in leaves of *Cucumis sativus* L. at low temperatures is photosystem I, not photosystem II. *Planta*, 193(2), 300–306. Available from: https://doi.org/10.1007/BF00192544

Tikhonov, A.N. (2023) The cytochrome b_6f complex: plastoquinol oxidation and regulation of electron transport in chloroplasts. *Photosynthesis Research*. Available from: https://doi.org/10.1007/s11120-023-01034-w

Tikhonov, A.N., Khomutov, G.B., Ruuge, E.K. & Blumenfeld, L.A. (1981) Electron transport control in chloroplasts; effects of photosynthetic control monitored by the intrathylakoid pH. *Biochimica et Biophysica Acta (BBA)—Bioenergetics*, 637(2), 321–333. Available from: https://doi.org/10.1016/0005-2728(81)90171-7

Tjus, S.E., Lindberg Møller, B. & Vibe Scheller, H. (1998) Photosystem I is an early target of photoinhibition in barley illuminated at chilling temperatures. *Plant Physiology*, 116(2), 755–764. Available from: https://doi.org/10.1104/pp.116.2.755

Vialet-Chabrand, S., Matthews, J.S.A., Simkin, A.J., Raines, C.A. & Lawson, T. (2017) Importance of fluctuations in light on plant photosynthetic acclimation. *Plant Physiology*, 173(4), 2163–2179. Available from: https://doi.org/10.1104/pp.16.01767

Wada, S., Amako, K. & Miyake, C. (2021) Identification of a novel mutation exacerbated the PSI photoinhibition in pgr5/pgrl1 mutants; caution for overestimation of the phenotypes in Arabidopsis pgr5-1 mutant. *Cells*, 10(11), 2884. Available from: https://doi.org/10.3390/cells10112884

Wang, C., Yamamoto, H. & Shikanai, T. (2015) Role of cyclic electron transport around photosystem I in regulating proton motive force. *Biochimica et Biophysica Acta (BBA)—Bioenergetics*, 1847(9), 931–938. Available from: https://doi.org/10.1016/j.bbabio.2014.11.013

Ware, M.A., Belgio, E. & Ruban, A.V. (2015) Comparison of the protective effectiveness of NPQ in Arabidopsis plants deficient in PsbS protein and zeaxanthin. *Journal of Experimental Botany*, 66(5), 1259–1270. Available from: https://doi.org/10.1093/jxb/eru477

Way, D.A. & Pearcy, R.W. (2012) Sunflecks in trees and forests: from photosynthetic physiology to global change biology. *Tree Physiology*, 32(9), 1066–1081. Available from: https://doi.org/10.1093/treephys/tps064

Wei, Z., Duan, F., Sun, X., Song, X. & Zhou, W. (2021) Leaf photosynthetic and anatomical insights into mechanisms of acclimation in rice in response to long-term fluctuating light. *Plant, Cell & Environment*, 44(3), 747–761. Available from: https://doi.org/10.1111/pce.13954

Yamamoto, H., Peng, L., Fukao, Y. & Shikanai, T. (2011) An Src homology 3 domain-like fold protein forms a ferredoxin binding site for the chloroplast NADH dehydrogenase-like complex in Arabidopsis. *The Plant Cell*, 23(4), 1480–1493. Available from: https://doi.org/10.1105/tpc.110.080291

Yamamoto, H. & Shikanai, T. (2019) PGR5-dependent cyclic electron flow protects photosystem I under fluctuating light at donor and acceptor sides. *Plant Physiology*, 179(2), 588–600. Available from: https://doi.org/10.1104/pp.18.01343

Yamori, W., Makino, A. & Shikanai, T. (2016) A physiological role of cyclic electron transport around photosystem I in sustaining photosynthesis under fluctuating light in rice. *Scientific Reports*, 6, 20147. Available from: https://doi.org/10.1038/srep20147

Yamori, W., Sakata, N., Suzuki, Y., Shikanai, T. & Makino, A. (2011) Cyclic electron flow around photosystem I via chloroplast NAD(P)H dehydrogenase (NDH) complex performs a significant physiological role during photosynthesis and plant growth at low temperature in rice. *The Plant Journal*, 68(6), 966–976. Available from: https://doi.org/10.1111/j.1365-313X.2011.04747.x

Yamori, W. & Shikanai, T. (2016) Physiological functions of cyclic electron transport around photosystem I in sustaining photosynthesis and plant growth. *Annual Review of Plant Biology*, 67, 81–106. Available from: https://doi.org/10.1146/annurev-arplant-043015-112002

Yamori, W., Shikanai, T. & Makino, A. (2015) Photosystem I cyclic electron flow via chloroplast NADH dehydrogenase-like complex performs a physiological role for photosynthesis at low light. *Scientific Reports*, 5, 13908. Available from: https://doi.org/10.1038/srep15593

Zhou, Q., Yamamoto, H. & Shikanai, T. (2022) Distinct contribution of two cyclic electron transport pathways to P700 oxidation. *Plant Physiology*, 192(1), 326–341. Available from: https://doi.org/10.1093/plphys/kiac557

SUPPORTING INFORMATION

Additional supporting information can be found online in the Supporting Information section at the end of this article.

How to cite this article: Niu, Y., Matsubara, S., Nedbal, L. & Lazár, D. (2024) Dynamics and interplay of photosynthetic regulatory processes depend on the amplitudes of oscillating light. *Plant, Cell & Environment*, 47, 2240–2257. https://doi.org/10.1111/pce.14879